Nanomechanics of Organic Layers and Biomenbranes

Gerard Oncins Marco

Universitat de Barcelona

Facultat de Química

Departament de Química Física

NANOMECHANICS OF ORGANIC LAYERS AND BIOMEMBRANES

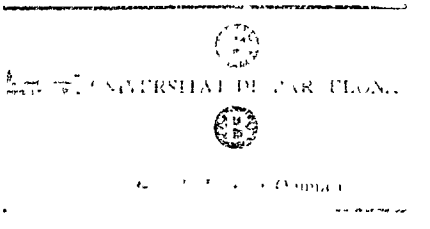

Gerard Oncins Marco

TESI DOCTORAL

Invited Paper

Nanomechanical Properties of Supported Lipid Bilayers studied by Force Spectroscopy

Sergi Garcia-Manyes, Gerard Oncins, and Fausto Sanz
Department of Physical Chemistry, Universitat de Barcelona, 08028 Barcelona, Spain

ABSTRACT

The physicochemical properties of biological membranes are crucial to understand membrane function, since their main role is to provide a barrier that divides electrolytic solutions into different compartments guaranteeing at the same time membrane mechanical stability. It is well-known that the chemical composition of the phospholipid molecules that compose the membrane greatly determine the architecture of such biological systems.

Force Spectroscopy with AFM is a powerful tool able to study the nanomechanical properties of supported planar bilayers (SPBs). Force plots on lipid bilayers show a discontinuity in the approaching curve that is interpreted as the penetration of the AFM tip through the lipid bilayer. The force at which this discontinuity occurs is the maximum force the bilayer is able to withstand before breaking and it can be regarded as a "fingerprint" of the bilayer stability, just like force is the fingerprint for a protein to unfold or for a hard material surface to be indented. We report on an experimental quantitative Force Spectroscopy study on how both lipid bilayer stability and compactness depend on the solution ionic composition.

1. INTRODUCTION

Due to its high biological relevance, many efforts have been devoted to the study of physicochemical properties of lipid bilayers in the last years, since they are crucial in order to understand specific membrane function. Lipid bilayers have been often studied in solution in their liposome form. It is widely known that in contact with a surface, those liposome break and spontaneously adsorb to a planar solid support thus creating a single lipid bilayer[1,2]. Hence the name of supported planar lipid bilayers (SPBs). In fact, SPBs are known to correctly mimic up to an extent complex biological membranes[3] and have been used as model membranes to study cell-cell recognition in the immune system, adhesion of cells, phospholipid diffusion, protein binding to lipid ligands and membrane insertion of proteins[4,5]. Atomic force microscopy has allowed to understand how supported planar lipid bilayers (SPBs) assemble and which are the interaction forces that act between vesicle and substrate surfaces and also between membrane surfaces, which is fundamental to efforts in chemistry, structural biology, and biophysics[1,6]. By imaging lipid bilayers in aqueous media with AFM both molecular structure and morphological aspects have been demonstrated[7-10]. Besides imaging, force spectroscopy allows to obtain valuable experimental information about the interaction forces and mechanical behavior of the studied systems with nanometric and nanonewton resolution through the force-distance curves[11]. When performing force curves on molecular thin films, a jump of the tip towards the surface is often observed once a threshold force has been exceeded. These jumps have been also observed in various systems such as surfactant layers on substrates[12], indicating tip penetration through the film, i.e., film rupture. Jumps on the force plots have also been observed when dealing with confined liquids, corresponding to a layer-by-layer tip penetration through the well-ordered squeezed liquid film[13-16] and also upon alkali halide single crystal nanoindentation, in which the tip penetrates the surface in a discrete layer-by-layer process[17]. Recalling lipid bilayers, force-curves have allowed to obtain valuable information regarding phospholipid interaction forces, such as those generated either by DLVO forces, by hydration forces or by steric forces[18]. Recent contributions have dealt with membrane nanomechanics using Force Spectroscopy, especially regarding the measurement of the elastic/plastic behaviour of the bilayer as a function of its composition, or the interaction with chemically modified probes[9,18,19]. Like in the case of other thin films, a jump on the approaching force curve has also been also reported, this breakthrough being interpreted as the penetration of the AFM tip through the lipid bilayer[20]. The force at which this jump in the force plot occurs is the maximum force the bilayer is able to withstand before breaking. Therefore, a quantitative measurement of the force at which the jump occurs can shed light on to acquiring basic information concerning cell membrane nanomechanics as well as interaction forces between neighboring lipid molecules in the membrane. The effects of some of the factors (variables) involved in membrane stability can be therefore assessed through this jump in the force plot thanks to those force spectroscopy measurements. Likewise, the force at which this

Smart Materials IV, edited by Nicolas H. Voelcker, Proc. of SPIE Vol. 6413, 64130E, (2006)
0277-786X/06/$15 · doi: 10.1117/12.697228

jump occurs can be regarded as a «fingerprint» of the bilayer stability under the experimental conditions the measurement is performed, just like force is the fingerprint for a protein to unfold or for a hard material surface to be indented. The yield threshold determination can then account for the overall forces that bind neighboring phospholipids together.

Controlling the involved variables can result in a better understanding of the regulating processes that nature can use to govern cell membrane interactions. So far, the dependence of the yield threshold force with the tip chemistry has been studied. It has been demonstrated that while hydrophilic tips yield a high breakthrough force, hydrophobic tips give rise to a breakthrough force near the contact force [19]. Besides, the approaching tip velocity has also been shown to have an effect on the force value at which the yield threshold occurs: the greater the tip approaching velocity, the higher force the jump will occur, as a quantitative model predicts[21,22]. However, even though those parameters have started being studied, there are three fundamental issues that have not been elucidated so far: i) the effect of phospholipid chemical structure and ii) the effect of the ionic strength of the measuring media.

Regarding i), a first approach has been reported[18,19], but there are still some questions lacking answer: is the polar head in the phospholipid molecule the main responsible for the bilayer nanomechanics? Or does the hydrophobic tail play also an important role? And further: Does the degree of insaturation play also a role on the compactness of the bilayer?

Concerning ii) we have to take into account that the main biological role of bilayers is to provide a barrier that divides electrolytic solutions into different compartments. Therefore, the effect of electrolytic solutions on membranes is of great importance and has deserved wide research[23]. Besides, ion binding affects the stability of proteins and their binding process to membranes[24] and it is also the main responsible for lipid vesicle fusion[25,26]. From an experimental point of view, many works, especially in the 1980's have dealt with the quantification of membrane surface potential through the electrophoretic mobility of lipid membranes under solutions with different ionic strength allowing the calculation of the ξ-potential value[27,28]. More recently, contributions regarding IR[24] and fluorescent techniques have also helped to shed light onto this issue. Finally, recent molecular dynamics simulations have allowed to understand the underlying processes from an atomistic point of view and have helped to study the role that cations play upon membrane structure and stability[29-31]. Indeed, we know that electrostatic interactions govern structural and dynamical properties of many biological systems[32,33]. In the case of phospholipid bilayers, the role of monovalent ions (e.g. Na^+) seems to have been so far underestimated, as theoretical simulations seem to predict. Indeed, MD Simulations[31,34] suggest a strong interaction between sodium and calcium ions and the carbonyl oxygens of the lipids, thus forming tight ion-lipid complexes giving rise to a higher degree of membrane organization. Likewise, the lateral interaction between the phospholipids molecules increases with the overall result of a more efficient packing (reduction of the area per lipid value) of the phospholipid structure. Since natural lipid membranes are composed of different phospholipid molecules in a wide range of concentrations, it is always difficult to assess the contribution of every type of phospholipid to the total nanomechanical response of the system. The role of ionic strength can be tested on all phospholipid systems, even though for the sake of simplicity and to start with we have firstly dealt with model lipid membranes such as 1, 2-Dimyristoyl-*sn*-glycero-3-phosphatidylcholine (DMPC), 1,2-Dilauroyl-*sn*-glycero-3-Phosphocholine (DLPC) and 1,2-Dipalmitoyl-*sn*-glycero-3-Phosphocholine (DPPC) deposited on mica. Later on, the study has been extended to a phosphatidylethanolamine (PE) bilayer, and finally, the nanomechanical response of a natural lipid bilayer has been studied. The goal of this work is mainly to perform an experimental quantitative force spectroscopy detailed approach to understand the nanomechanics of lipid bilayers and the forces involved in membrane deformation and failure in aqueous environment, especially dealing with the role of ionic strength on the nanomechanical response of the membrane.

2. EXPERIMENTAL

2.1 Sample preparation

1,2-Dimyristoyl-*sn*-glycero-3-phosphocholine (DMPC, Sigma, > 98 %) was dissolved in chloroform/ethanol (3:1) (Carlo Erba, analysis grade, at 99.9 %) to give a final DMPC concentration of 2 mM. This dissolution was kept at –10 °C. A 500 µl aliquote was poured in a glass vial and the solvent was evaporated with a nitrogen flow, obtaining a DMPC film at the bottom of the vial. Solution was kept in vacuum overnight to ensure the absence of organic solvent traces. Then, aqueous solution at the correct ionic strength was added until a final DMPC concentration of 500 µM and 0 mM

NaCl, 50 mM NaCl, 75 mM NaCl,100 mM NaCl and 150 mM NaCl + 20 mM $MgCl_2$ dissolutions respectively. All solutions used in the present work were set at pH = 7.4 with 10 mM Hepes/NaOH. Because of the low solubility of DMPC in water, the vial was subjected to 30 second cycles of vortexing, temperature and sonication until the obtention of a homogeneous mixture. The solution was finally sonicated for 20 minutes (in order to have unilamellar liposomes) and let it settle overnight always protected from light and maintained at 4 °C. Prior to its use, mica surfaces (Metafix, CLLS grade) were glued onto teflon discs with a water insoluble mounting wax. 50 µl of DMPC dissolution at the specific NaCl concentration were applied to cover 0.5 cm^2 freshly cleaved piece of mica for a deposition time of 35 min. After that, mica was rinsed three times with 100 µl of the corresponding ionic aqueous solution.

2.2 Zeta potential measurements

ξ-potential measurements were performed with a Zetamaster Particle Electrophoresis Analyser through which the velocity of the particles can be measured with a light scattering technique by using the Doppler effect thanks to a pair of mutually coherent laser beams (5 mW, He-Ne laser @ 633 nm). Zetamaster measures the autocorrelation function of the scattered light and after the signal processing it obtains the electrophoretic mobility and, finally, through the Henry equation, the ξ-potential.

2.3 AFM imaging

AFM images were acquired with a Dimension 3100 (Digital Instruments, Santa Barbara) microscope controlled by a Nanoscope IV electronics (Digital Instruments, CA) in contact mode using V-shaped Si_3N_4 tips (OMCL TR400PSA, Olympus, Japan) cantilevers. The applied force was controlled by acquiring force plots before and after every image was captured so as to measure the distance from the set point value.

2.4 Force spectroscopy

Force spectroscopy was performed with a Molecular Force Probe 1-D (MFP), Asylum Research (Santa Barbara, CA). Force plots were acquired using V-shaped Si_3N_4 tips (OMCL TR400PSA, Olympus, Japan) with a nominal spring constant of 0.08 N/m. Individual spring constants were calibrated using the equipartition theorem (thermal noise)[19] after having correctly measured the piezo sensitivity [V/nm] by measuring it at high voltages after several minutes of performing force plots to avoid hysteresis. It has to be pointed out that the results here shown for DMPC bilayers were obtained with the same cantilever keeping the spot laser at the same position on the lever to avoid changes in the spring constant calculation [50]. However, results have low scattering when using different tips and different samples. About 1300 curves over more than 15 positions were obtained for each sample. All force spectroscopy and AFM images were obtained at 20 °C ± 0.5 °C. which is below the main phase transition temperature (T_M) of DMPC (23.5 °C). Besides, we have to consider here that T_M for supported bilayers shifts to a higher temperature than observed in solution [51]. Therefore, we are indenting the gel phase for DMPC supported bilayers. Applied forces F are given by $F = k_c X \Delta$ where Δ is the cantilever deflection. The surface deformation is given as penetration δ (evaluated as $\delta = z - \Delta$, where z represents the piezo-scanner displacement.

2.5 DSC measurements

DSC measurements were performed with a MicroCal MC-2 (MicroCal, Inc., Northhampton, MA). The heating and cooling rate was usually 10 °C h^{-1} and the measurements were performed in the temperature interval from 10 to 55 °C. The reproducibility of the DSC experiments was checked by three consecutive scans of each sample.

3. RESULTS

3.1 Effect of ion-binding (ionic strength) on the nanomechanics of lipid bilayers. DMPC model membrane

Recent molecular dynamics simulations show the tendency of phosphatidylcholine (PC) head to adsorb cations. Contrary to early experimental measurements, where only divalent cations such as Mg2+ and Ca2+ were found to effectively bound to the phospholipid surface52, Na+ has also been recently proved to bind into the membranes, both from theoretical calculations, concerning 1-Palmitoyl-2-Oleoyl-sn-3-Phosphocholine (POPC)31,34, DPPC29, and also experimentally31,53. MD simulations predict a coordination of cations to the PC lipid carbonyl oxygens, yielding coordination numbers of 2.9 for Na+ and 4.2 for Ca2+, the latter in a sequential binding process34. These findings foresee a change both in the structure and dynamical properties of zwitterionic lipid bilayer to a previously unexpected extent. A first experimental approach to study ion adsorption on the membrane is the measurement of the liposome mobility in an electrophoretic field and likewise measuring the ξ-potential. Although the zeta potential value does not yield directly the surface charge, but the charge at the point where the Stern layer and the diffuse layer meet (shear plane), it is considered to yield a significant approximation of the surface potential. Figure 1 shows the evolution of the ξ-potential value of a DMPC unilamellar liposome solution as the ionic strength of the solution is increased. All concentrations refer only to NaCl addition, but for the last point in the graph, in which 20 mM MgCl2 have been added to a 150 mM NaCl solution in order to mimic physiological concentrations.

As the ionic strength increases, the net ξ-potential value increases, reflecting that indeed positive cations may adsorb on the surface of the polar head of the phospholipid molecule. It is widely accepted that most natural membranes are negatively charged because of the presence of variable quantities of negatively charged phospholipids, yielding surface charges on the order of -0.05 C/m^2. However, in this case, we have to take into account that even though PC heads are zwitterionic and thus theoretically globally uncharged at neutral pH, it gives rise to a negative ξ-potential value (-12.0 ± 1.6 mV) in mQ water. This has been interpreted in terms of hydration layers formed around the surface[53] and to the orientation of lipid headgroups[28].

The process of vesicle fusion to a flat bilayer is assumed to be electrostatically governed, and that surface free energy plays a key role[54]. Freshly cleaved mica is negatively charged upon a wide range of ionic strength[53], so that according to figure 1 the higher the ionic strength, the higher and the faster the adhesion of DMPC liposomes onto mica surface will be. This process will be especially favored at high ionic strength, where the surface zeta potential is positive (6.86 ± 2.3 mV). The probable divalent cation preference for membrane binding may also help to reverse the obtained net zeta potential value (from negative values to positive values). Figure 2 shows AFM contact mode images of DMPC bilayers as the ionic strength of the surface is increased, showing that the degree of surface coverage is strongly dependent on the amount of ions present in the system. Fig 2a shows a 5×5 μm^2 contact mode image of DMPC bilayer in distilled water; fig. 2b in 50 mM NaCl and fig. 2c shows a 7.5×7.5 μm^2 image of DMPC in 150 mM NaCl + 20 mM $MgCl_2$ 10. Fig 2c.1 shows a cross section of the marked area in Fig 2c in which, thanks to the surface defects, the bilayer height can be measured to be ~ 4.5 nm.

A series of 500 μM DMPC solution in Millipore water with different ionic strengths (0 mM, 50 mM, 75 mM and 100 mM NaCl or 150 mM NaCl + 20 mM $MgCl_2$, all of them with 10 mM Hepes, pH = 7.4) were deposited onto a freshly cleaved mica surface and mounted on a Molecular Force Probe 1-D (MFP) liquid cell.

Force curves (fig. 3) exhibit a breakthrough feature (black arrows) in the approaching curve (red line) corresponding to the penetration of the bilayer by the tip apex and indicating that the lipid bilayer is not able to withstand the force exerted by the tip. Concerning the retracting curve (blue line) we observe an adhesion peak, which corresponds to the adhesion between the silicon nitride tip and the surface. The width of the jump (~4.5 nm) corresponds to the height of the bilayer, (cross section in figure 2c.1). In figure 3a) the breakthrough force (also called yield threshold force value) occurs at ~15 nN. This curve has been taken in a 150 mM NaCl + 20 mM $MgCl_2$ solution. In figure 3b), the force plot was taken on a DMPC bilayer in distilled water and the yield threshold is found at ~2.2 nN, which is about 7 fold lower.

Fig 4 shows the histograms of the yield threshold force values ranging from 2.76 ± 0.11 nN in pure water to 14.93 ± 0.09 nN in buffered high ionic strength solution. Those histograms have been obtained taking only the successful indentation recordings (we call a successful recording the one that presents a breakthrough in the force plot). As we have

already clearly seen in figure 2, the higher the ionic strength, the higher the degree of coverage of the surface. Thus, the probability of a successful recording is higher as we increase the ionic strength of the solution. In the cases in which the bilayer presents uncovered regions (e.g. figures 2a and 2b) when an unsuccessful force plot occurs it means that we are attempting on an «empty» area, and we normally observe a typical silicon nitride-bare mica force plot.

4. CONCLUSIONS

Concerning the role of ionic strength on the nanomechanics of lipid bilayers, we have reported on a detailed experimental quantitative Force Spectroscopy study on how ion binding affects upon model PC lipid membrane nanomechanics. We have experimentally proved that the higher the ionic strength, the higher the force that has to be applied with the AFM tip in order to penetrate the bilayer. These results are in agreement with recent works that have demonstrated both experimentally and theoretically that cations (both monovalent, e.g. Na^{+}, and divalent, e.g. Ca^{2+}) penetrate the headgroups of phospholipids molecules giving rise to a more packed phospholipid network and a higher phospholipid-phospholipid lateral interaction. This increase in lateral interaction between neighboring molecules may be the cause for the extension of the elastic deformation region in the force plots before the onset of plastic region (yield threshold force value).

Summarizing, this work opens a new investigation line dealing with the relationship between the experimental measurements regarding the nanomechanics of membranes in the nanometer/nanonewton range and the atomic underlying processes. This is an interesting example of how (small) variations in chemical composition both in chemical structure and in the surrounding media can translate into (considerable) variations in the (nano)mechanical response of the membrane system.

5. REFERENCES

1. Leonenko, Z. V.; Carnini, A.; Cramb, D. T., "Supported planar bilayer formation by vesicle fusion: the interaction of phospholipid vesicles with surfaces and the effect of gramicidin on bilayer properties using atomic force microscopy", Biochim.Biophys.Acta, **1509**, 131-147, 2000.

2. Jass, J.; Tjarnhage, T.; Puu, G., "From liposomes to supported, planar bilayer structures on hydrophilic and hydrophobic surfaces: An atomic force microscopy study", Biophysical Journal, **79**, 3153-3163, 2000.

3. Sackmann, E., "Supported membranes: scientific and practical applications", Science, **271**, 43-48, 1996.

4. Mueller, H.; Butt, H. J.; Bamberg, E., "Adsorption of membrane-associated proteins to lipid bilayers studied with an atomic force microscope: Myelin basic protein and cytochrome c", Journal of Physical Chemistry B, **104**, 4552-4559, 2000.

5. Desmeules, P.; Grandbois, M.; Bondarenko, V. A.; Yamazaki, A.; Salesse, C., "Measurement of membrane binding between recoverin, a calcium-myristoyl switch protein, and lipid bilayers by AFM-based force spectroscopy", Biophys.J., **82**, 3343-3350, 2002.

6. Benz, M.; Gutsmann, T.; Chen, N.; Tadmor, R.; Israelachvili, J., "Correlation of AFM and SFA measurements concerning the stability of supported lipid bilayers", Biophys.J., **86**, 870-879, 2004.

7. Kaasgaard, T.; Leidy, C.; Ipsen, J. H.; Mouritsen, O. G.; Jorgensen, K., "In situ atomic force microscope imaging of supported lipid bilayers", Single Molecules, **2**, 105-108, 2001.

8. Slade, A.; Luh, J.; Ho, S.; Yip, C. M., "Single molecule imaging of supported planar lipid bilayer--reconstituted human insulin receptors by in situ scanning probe microscopy", J.Struct.Biol., **137**, 283-291, 2002.

9. Schneider, J.; Barger, W.; Lee, G. U.. "Nanometer scale surface properties of supported lipid bilayers measured with hydrophobic and hydrophilic atomic force microscope probes", Langmuir, **19**, 1899-1907, 2003.

10. Seantier, B.; Breffa, C.; Felix, O.; Decher, G.. "In situ investigations of the formation of mixed supported lipid bilayers close to the phase transition temperature", Nano Letters, **4**, 5-10, 2004.

11. Weisenhorn, A. L.; Maivald, P.; Butt, H. J.; Hansma, P. K., "Measuring Adhesion, Attraction, and Repulsion Between Surfaces in Liquids with An Atomic-Force Microscope", Physical Review B, **45**, 11226-11232, 1992.

12. Jaschke, M.; Butt, H. J.; Gaub, H. E.; Manne, S., "Surfactant aggregates at a metal surface", Langmuir, **13**, 1381-1384, 1997.

13. O'Shea, S. J. and Welland, M. E., "Atomic force microscopy at solid-liquid interfaces", Langmuir, **14**, 4186-4197, 1998.

14. Oshea, S. J.; Welland, M. E.; Rayment, T., "Solvation Forces Near A Graphite Surface Measured with An Atomic Force Microscope", Applied Physics Letters, **60**, 2356-2358, 1992.

15. Franz, V. and Butt, H. J., "Confined liquids: Solvation forces in liquid alcohols between solid surfaces", Journal of Physical Chemistry B, **106**, 1703-1708, 2002.

16. Sun, G. X.; Bonaccurso, E.; Franz, V.; Butt, H. J., "Confined liquid: Simultaneous observation of a molecularly layered structure and hydrodynamic slip", Journal of Chemical Physics, **117**, 10311-10314, 2002.

17. Fraxedas, J.; Garcia-Manyes, S.; Gorostiza, P.; Sanz, F., "Nanoindentation: Toward the sensing of atomic interactions", Proceedings of the National Academy of Sciences of the United States of America, **99**, 5228-5232, 2002.

18. Dufrene, Y. F.; Boland, T.; Schneider, J. W.; Barger, W. R.; Lee, G. U., "Characterization of the physical properties of model biomembranes at the nanometer scale with the atomic force microscope", Faraday Discuss., 79-94, 1998.

19. Richter, R. P. and Brisson, A., "Characterization of lipid bilayers and protein assemblies supported on rough surfaces by atomic force microscopy", Langmuir, **19**, 1632-1640, 2003.

20. Franz, V.; Loi, S.: Muller, H.; Bamberg, E.; Butt, H. H., "Tip penetration through lipid bilayers in atomic force microscopy", Colloids and Surfaces B-Biointerfaces, **23**, 191-200, 2002.

21. Loi, S.; Sun, G.; Franz, V.; Butt, H. J., "Rupture of molecular thin films observed in atomic force microscopy. II. Experiment", Physical Review E, **66**, 2002.

22. Butt, H. J. and Franz, V., "Rupture of molecular thin films observed in atomic force microscopy. I. Theory", Physical Review E, **66**, 2002.

23. Cevc, G., "Membrane electrostatics", Biochim.Biophys.Acta, **1031**, 311-382, 1990.

24. Binder, H. and Zschornig, O., "The effect of metal cations on the phase behavior and hydration characteristics of phospholipid membranes", Chem.Phys.Lipids, **115**, 39-61, 2002.

25. Ohki, S.; Duzgunes, N.; Leonards, K., "Phospholipid vesicle aggregation: effect of monovalent and divalent ions", Biochemistry, **21**, 2127-2133, 1982.

26. Ohki, S.; Roy, S.; Ohshima, H.; Leonards, K., "Monovalent cation-induced phospholipid vesicle aggregation: effect of ion binding", Biochemistry, **23**, 6126-6132, 1984.

27. Eisenberg, M.; Gresalfi, T.; Riccio, T.; McLaughlin, S., "Adsorption of monovalent cations to bilayer membranes containing negative phospholipids", Biochemistry, **18**, 5213-5223, 1979.

28. Makino, K.; Yamada, T.; Kimura, M.; Oka, T.; Ohshima, H.; Kondo, T., "Temperature- and ionic strength-induced conformational changes in the lipid head group region of liposomes as suggested by zeta potential data", Biophys.Chem., **41**, 175-183, 1991.

29. Pandit, S. A.; Bostick, D.; Berkowitz, M. L., "Molecular dynamics simulation of a dipalmitoylphosphatidylcholine bilayer with NaCl", Biophys.J., **84**, 3743-3750, 2003.

30. Pandit, S. A.; Bostick, D.; Berkowitz, M. L., "Mixed bilayer containing dipalmitoylphosphatidylcholine and dipalmitoylphosphatidylserine: lipid complexation, ion binding, and electrostatics", Biophys.J., **85**, 3120-3131, 2003.

31. Bockmann, R. A.; Hac, A.; Heimburg, T.; Grubmuller, H., "Effect of sodium chloride on a lipid bilayer", Biophys.J., **85**, 1647-1655, 2003.

32. Thompson, J. B.; Kindt, J. H.; Drake, B.; Hansma, H. G.; Morse, D. E.; Hansma, P. K., "Bone indentation recovery time correlates with bond reforming time", Nature, **414**, 773-776, 2001.

33. Ratanabanangkoon, P. and Gast, A. P., "Effect of ionic strength on two-dimensional streptavidin crystallization", Langmuir, **19**, 1794-1801., 2003.

34. Bockmann, R. A. and Grubmuller, H., "Multistep binding of divalent cations to phospholipid bilayers: a molecular dynamics study", Angew.Chem.Int.Ed Engl., **43**, 1021-1024, 2004.

35. Nagle, J. F. and Tristram-Nagle, S., "Structure of lipid bilayers", Biochimica et Biophysica Acta-Reviews on Biomembranes, **1469**, 159-195, 2000.

36. Nagle, J. F.; Petrache, H. I.; Gouliaev, N.; Tristram-Nagle, S.; Liu, Y. F.; Suter, R. M.; Gawrisch, K., "Multiple mechanisms for critical behavior in the biologically relevant phase of lecithin bilayers", Physical Review E, **58**, 7769-7776, 1998.

37. Wu, S. H. W. and M^{c}Connel, H. M, "Lateral Phase Separations and Perpendicular Transport in Membranes", Biochemical and Biophysical Research Communications, **55**, 484-491, 1973.

38. Papahadj.D; Jacobson, K.; Nir, S.; Isac, T., "Phase-Transitions in Phospholipid Vesicles - Fluorescence Polarization and Permeability Measurements Concerning Effect of Temperature and Cholesterol", Biochimica et Biophysica Acta, **311**, 330-348, 1973.

39. Pope, J. M.; Walker, L.; Cornell, B. A.; Francis, G. W., "Nmr-Study of Synthetic Lecithin Bilayers in the Vicinity of the Gel-Liquid-Crystal Transition", Biophysical Journal, **35**, 509-520, 1981.

40. Pabst, G.; Katsaras, J.; Raghunathan, V. A.; Rappolt, M., "Structure and interactions in the anomalous swelling regime of phospholipid bilayers", Langmuir, **19**, 1716-1722, 2003.

41. Ge, M. and Freed, J. H., "Hydration, structure, and molecular interactions in the headgroup region of dioleoylphosphatidylcholine bilayers: an electron spin resonance study", Biophys.J., **85**, 4023-4040, 2003.

42. Schneider, J.; Dufrene, Y. F.; Barger, W. R., Jr.; Lee, G. U., "Atomic force microscope image contrast mechanisms on supported lipid bilayers", Biophys.J., **79**, 1107-1118, 2000.

43. Leonenko, Z. V.; Finot, E.; Ma, H.; Dahms, T. E.; Cramb, D. T., "Investigation of temperature-induced phase transitions in DOPC and DPPC phospholipid bilayers using temperature-controlled scanning force microscopy", Biophys.J., **86**, 3783-3793, 2004.

44. Giocondi, M. C. and Le Grimellec, C., "Temperature dependence of the surface topography in dimyristoylphosphatidylcholine/distearoylphosphatidylcholine multibilayers", Biophysical Journal, **86**, 2218-2230, 2004.

45. Enders, O.; Ngezahayo, A.; Wiechmann, M.; Leisten, F.; Kolb, H. A., "Structural calorimetry of main transition of supported DMPC billayers by temperature-controlled AFM", Biophysical Journal, **87**, 2522-2531, 2004.

46. Tokumasu, F.; Jin, A. J.; Dvorak, J. A., "Lipid membrane phase behaviour elucidated in real time by controlled environment atomic force microscopy", Journal of Electron Microscopy, **51**, 1-9, 2002.

47. Giocondi, M. C.; Pacheco, L.; Milhiet, P. E.; Le Grimellec, C., "Temperature dependence of the topology of supported dimirystoyl-distearoyl phosphatidylcholine bilayers", Ultramicroscopy, **86**, 151-157, 2001.

48. Newman, M. J. and Wilson, T. H., "Solubilization and reconstitution of the lactose transport system from Escherichia coli", J.Biol.Chem., **255**, 10583-10586, 1980.

49. Florin, E. L.; Rief, M.; Lehmann, H.; Ludwig, M.; Dornmair, C.; Moy, V. T.; Gaub, H. E., "Sensing Specific Molecular-Interactions with the Atomic-Force Microscope", Biosensors & Bioelectronics, **10**, 895-901, 1995.

50. Proksch, R.; Schäffer, T. E.; Cleveland, J. P.; Callahan, R. C.; Viani, M. B., "Finite optical spot size and position corrections in thermal spring constant calibration", Nat.Struct.Biol., **15**, 1344-1350, 2005.

51. Yang, J. and Appleyard, J., "The main phase transition of mica-supported phosphatidylcholine membranes", Journal of Physical Chemistry B, **104**, 8097-8100, 2000.

52. Marra, J. and Israelachvili, J., "Direct measurements of forces between phosphatidylcholine and phosphatidylethanolamine bilayers in aqueous electrolyte solutions", Biochemistry, **24**, 4608-4618, 1985.

53. Egawa, H. and Furusawa, K., "Liposome adhesion on mica surface studied by atomic force microscopy", Langmuir, **15**, 1660-1666, 1999.

54. Silin, V. I.; Wieder, H.; Woodward, J. T.; Valincius, G.; Offenhausser, A.; Plant, A. L., "The role of surface free energy on the formation of hybrid bilayer membranes", Journal of the American Chemical Society, **124**, 14676, 2002.

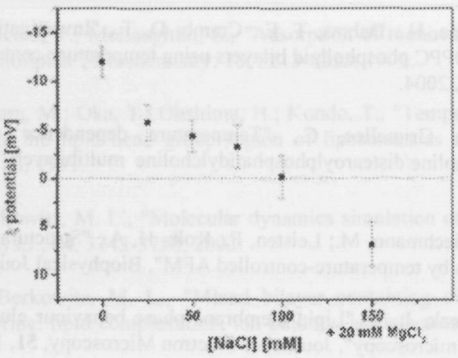

FIGURE 1. ξ-potential values of the DMPC liposomes vs. ionic strength of the measuring solution. Every point in the graph is the average of 15 independent measurements. Error bars stand for standard deviation value.

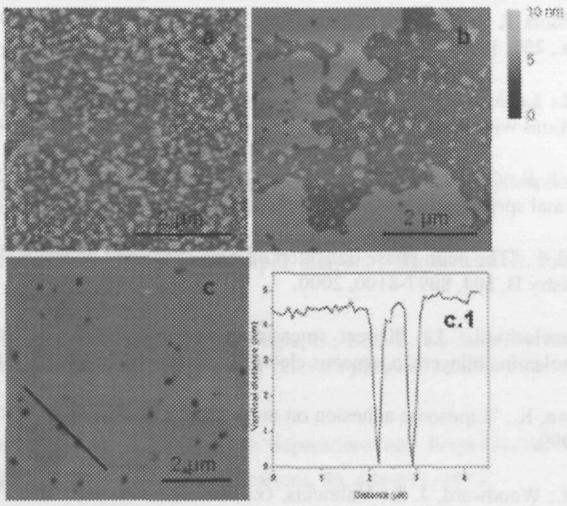

FIGURE 2. 5 × 5 µm2 AFM Contact Mode Images of DMPC bilayers in a) distilled water. b) 100 mM NaCl solution. c) 7 × 7 µm2 AFM Contact Mode Images of DMPC bilayer in 150 mM NaCl + 20 mM MgCl2. All solutions were buffered to pH = 7.4 with 10 mM Hepes/NaOH. c.1) Cross section profile of the marked area in figure c) All images have been taken after 35 minutes of liposome deposition.

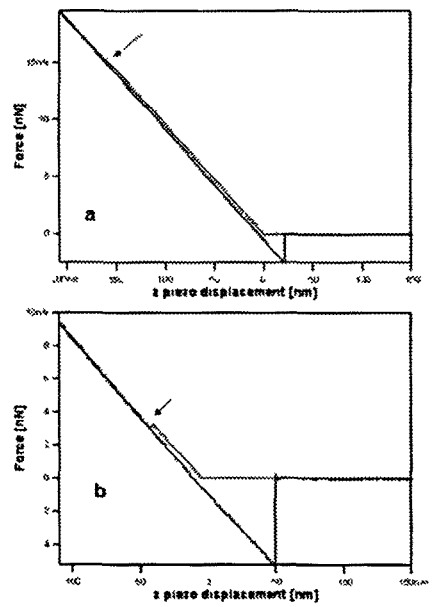

FIGURE 3. Force vs. z-piezo displacement plot for a DMPC bilayer in a) 150 mM NaCl + 20 mM $MgCl_2$ and b) distilled water. Yield threshold denoted by black arrows: a) ~15 nN and b) ~2.1 nN. The width of the jump, ~4.5 nm, corresponds well with the bilayer height measured using contact mode AFM.

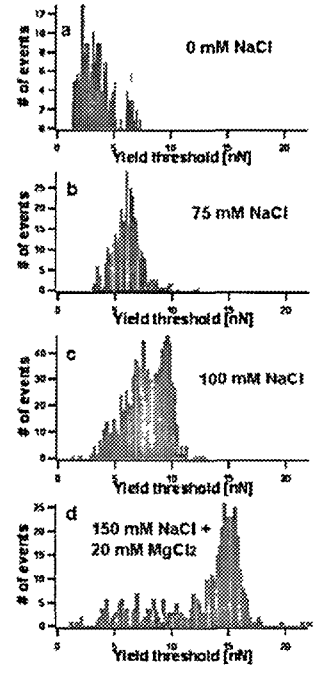

FIGURE 4. Histograms corresponding to the yield threshold force value for DMPC bilayers under different ionic composition: a) 0 mM NaCl, $x = 2.76 \pm 0.11$ nN ($N = 396$), b) 75 mM NaCl, $x = 6.04 \pm 0.01$ nN ($N = 568$), c) 100 mM NaCl, $x = 7.98 \pm 0.13$ nN ($N = 872$), d) 150 mM NaCl + 20 mM $MgCl_2$, $x = 14.93 \pm 0.09$ nN ($N = 427$). All results correspond to a Gaussian fitting of the data shown in the histogram. Results are presented as the Gaussian center $x \pm 2\sigma/\sqrt{N}$.

5.4.5 Effect of Temperature on the Nanomechanics of Lipid Bilayers studied by Force Spectroscopy

S. Garcia-Manyes, G. Oncins, F. Sanz

Department of Physical Chemistry, Universitat de Barcelona, Spain

Biophysical Journal 89, (2005), 4261-4274.

5.4.5.1 Summary

This project was born with two different goals in mind. First of all, the development of variable temperature AFM had opened new and exciting possibilities in the phospholipid bilayers research field and several groups were working on the in-situ topographic imaging of the main phase transition of SPBs in liquid environment. We had done quite a lot of work on PC bilayers and we also decided to go for it. Secondly, there was a rising interest about bilayer nanomechanics and Force Spectroscopy was becoming a key technique in the field, so studying the response of the bilayers during the phase transition process was an obvious thing to do because of the light Δx *vs.* Δz curves could shed on the somewhat obscure phase transition process. Our results can be summarized as follows:

- *The phase transition of two different PC bilayers was followed by variable temperature AFM and two phase transition were detected, both of them at a higher temperature that the liposomic* T_M. *This effect had been seen before and attributed to the stabilizing effect of the substrate.*

- *The* F_y *values obtained from the Force Spectroscopy experiments strongly depend on the temperature and on the bilayer phase. Then, for the* L_β *phase, the*

F_y value decreases as temperature increases, reaching a minimum around T_M. For higher temperatures (L_α phase), the F_y value increases slightly and reaches a plateau at vertical forces much lower than those obtained for the L_β phase. This behavior verifies for DMPC and 1,2-Dipalmitoyl-sn-Glycero-3-Phosphocholine (DPPC), although a different trend is observed for 1,2-Dilauroyl-sn-Glycero-3-Phosphocholine (DLPC) bilayers.

- *When I value is increased, the trend of F_y vs. temperature keeps on being the same, although it is shifted to higher F_y values.*

Biophysical Journal Volume 89 December 2005 4261–4274

Effect of Temperature on the Nanomechanics of Lipid Bilayers Studied by Force Spectroscopy

Sergi Garcia-Manyes, Gerard Oncins, and Fausto Sanz
Department of Physical Chemistry Universitat de Barcelona 08028 Barcelona Spain

ABSTRACT The effect of temperature on the nanomechanical response of supported lipid bilayers has been studied by force spectroscopy with atomic force microscopy We have experimentally proved that the force needed to puncture the lipid bilayer (F_y) is temperature dependent The quantitative measurement of the evolution of F_y with temperature has been related to the structural changes that the surface undergoes as observed through atomic force microscopy images These studies were carried out with three different phosphatidylcholine bilayers with different main phase transition temperature (T_M) namely 1,2-dimyristoyl-*sn*-glycero-3-phosphocholine, 1,2-dipalmitoyl-*sn*-glycero-3-phosphocholine, and 2-dilauroyl-*sn*-glycero-3-phosphocholine The solid-like phase shows a much higher F_y than the liquid-like phase which also exhibits a jump in the force curve Within the solid-like phase, F_y decreases as temperature is increased and suddenly drops as it approaches T_M Interestingly, a "well" in the F_y versus temperature plot occurs around T_M thus proving an "anomalous mechanical softening" around T_M Such mechanical softening has been predicted by experimental techniques and also by molecular dynamics simulations and interpreted in terms of water ordering around the phospholipid headgroups Ion binding has been demonstrated to increase F_y, and its influence on both solid and liquid phases has also been discussed

INTRODUCTION

Many efforts have been devoted to the study of physicochemical properties (1) of lipid bilayers in recent years since they are crucial to understanding specific membrane function Many of these structural and dynamic intrinsic bilayer properties such as the thickness of the bilayer, the area per lipid value, or the order parameter are governed by temperature (2) Indeed, lipid bilayers present many lamellar phases as a function of temperature, namely gel phase (L_β), liquid crystalline phase (L_α), subgel phase (L_c), and ripple phase (P_β) It is widely accepted that many biologically relevant processes occur in the liquid crystalline (L_α) phase, and therefore many works have focused on the study of structural and mechanical properties of this phase (2,3) Amid all the studies concerning phase transitions, the thermally induced gel-fluid transition has deserved special attention due to the large number of quantities that exhibit anomalous behavior near T_M, such as, e g , heat capacity, ζ-potential (4), electric conductivity (5), Na^+ permeability (6), NMR order parameter (7), swelling (8), or hydration behavior (9) Most of those studies have been performed in multilamellar liposome solutions In the case of supported planar phospholipid bilayers (SPBs), though, phospholipid molecules spontaneously adsorb to a planar solid support, thus creating a single lipid bilayer (10,11) In fact, SPBs are known to correctly mimic, up to an extent, complex biological membranes (12)

The atomic force microscope (AFM) has become an important tool to image supported thin films with nanometric resolution Concerning lipid bilayers, most of the studies have focused on resolving topographic characteristics in a liquid environment (13–22) With the possibility of accurately controlling temperature while scanning, a novel and promising research line has been opened, mainly devoted to studying topographic lipid bilayer surface features induced by temperature (23–28) Besides imaging, force spectroscopy allows us to obtain valuable experimental information about the interaction forces and mechanical behavior of the studied systems with nanometric and nanonewton resolution through the force-distance curves (29) When performing force curves in molecular thin films, a jump of the tip toward the surface is often observed once a threshold force has been exceeded These jumps have also been observed in various systems such as surfactant layers on substrates (30), indicating tip penetration through the film, i e , film rupture Jumps on the force plots have also been observed when dealing with confined liquids, corresponding to a layer-by-layer tip penetration through the well-ordered squeezed liquid film (31–34) and also upon alkali halide single crystal nanoindentation, in which the tip penetrates the surface in a discrete layer by layer process (35) Recalling lipid bilayers, force curves have allowed us to obtain valuable information regarding phospholipid interaction forces, such as those generated either by Derjaguin Landau Verwey-Overbeek forces, by hydration forces, or by steric forces (36) Recent contributions have dealt with membrane nanomechanics using force spectroscopy, especially regarding the measurement of the elastic/plastic behavior of the bilayer as a function of its composition or the interaction with chemically modified probes (16,36,37) As in the case of other thin films, a jump on the approaching force curve has also been reported, this breakthrough being interpreted as the

Submitted May 2 2005 and accepted for publication August 15 2005

Sergi Garcia Manyes and Gerard Oncins contributed equally to this work

Address reprint requests to Fausto Sanz Tel 34 934021240 Fax 34 934021231 E mail fsanz@ub edu

0006 3495/05/12/4261/14 $2 00

doi 10 1529/biophysj 105 065581

penetration of the AFM tip through the lipid bilayer (38). A quantitative measurement of the force at which the jump occurs can shed light onto gathering basic information concerning cell membrane nanomechanics as well as interaction forces between neighboring lipid molecules in the membrane. Therefore, the force value at which this jump takes place is closely related to membrane stability. So far, the dependence of the yield threshold force with the tip chemistry has been studied. It has been demonstrated that whereas hydrophilic tips yield a high material-dependent breakthrough force, hydrophobic tips give rise to a breakthrough force near the contact force (37). Besides, the approaching tip velocity has also been shown to have an effect on the force value at which the yield threshold occurs: the greater the tip approaching velocity, the higher the force within which the jump will occur, as a quantitative model predicts (39,40). Furthermore, in a recent work (1) we have shown that ionic strength increases the force at which the membrane breaks, probably due to ion binding on the phospholipid network, as a result of enhancing lateral interactions between neighboring molecules. This behavior was proved for model lecithin and phosphoethanolamine membranes as well as for natural membranes. Finally, in the framework of the same study, we correlated the yield threshold force with the chemical structure of both hydrophobic tails and hydrophilic heads. Likewise, the force at which this jump occurs can be regarded as a "fingerprint" of the bilayer stability under the experimental conditions in which the measurement is performed, just as force is the fingerprint for a protein to unfold or for a hard material surface to be indented. The yield threshold determination can then account for the overall forces that bind neighboring phospholipids together.

Temperature has a strong effect on lipid structure and stability. Therefore, the yield breakthrough, if present, should also present strong variations upon phase transition if it is really a direct mechanical reflection of molecular interactions. Although little work has been performed on this particular issue, it seems to be controversial (38) if the breakthrough can occur only in the solid-like phase (15) or the liquid-like phase (41). A pioneering meritorious publication (23) has suggested that the rupture force decreases as the temperature increases, but no quantitative experimental assessment has been reported.

In this work, we aim to perform a quantitative study of the dependence of the yield threshold force on model lipid bilayers with temperature and to relate the results with the structural changes that the surface undergoes as studied through AFM images. In particular, our first goal is to study whether the jump occurs in the gel phase, in the liquid phase, or in both. To this aim we have performed the same experiment with three different phosphatydilcholine phospholipids that exhibit a well-reported different main transition temperature, namely, 1,2-dipalmitoyl-*sn*-glycero-3-phosphocholine (DPPC), 1,2-dimyristoyl-*sn*-glycero-3-phosphocholine (DMPC), and 2-dilauroyl-*sn*-glycero-3-phosphocholine (DLPC). An in-depth study of the evolution of the yield threshold with temperature can shed light onto understanding the temperature-induced changes in the intermolecular interactions between the phospholipid molecules, which is crucial to many biological functions.

MATERIALS AND METHODS

Sample preparation

DMPC (Sigma St Louis, MO, >98%) was dissolved in chloroform/ethanol (3 1) (Carlo Erba, Milan, Italy, analysis grade, at 99 9%) to give a final DMPC concentration of 2 mM This solution was kept at – 10°C A 500 μl aliquot was poured into a glass vial, and the solvent was evaporated with a nitrogen flow obtaining a DMPC film at the bottom of the vial. Solution was kept in vacuum overnight to ensure the absence of organic solvent traces Then, water solution was added until a final DMPC concentration of 500 μM was obtained Because of the low solubility of DMPC in water, the vial was subjected to 30 s cycles of vortexing, temperature, and sonication until the mixture was homogeneous The solution was finally sonicated for 20 min (to have unilamellar liposomes) and allowed to settle overnight always protected from light and maintained at 4°C. Lipid resuspension was carried out by using either a high ionic strength solution (150 mM NaCl + 20 mM $MgCl_2$) or only distilled water All solutions used in this work were set at pH – 7 4 with 10 mM Hepes/NaOH Before its use, mica surfaces (Metafix, Montdidier, France) were glued onto Teflon discs with a water insoluble mounting wax A total of 50 μl of DMPC, DLPC or DPPC dissolution at the specific ionic strength was applied to cover 0 5 cm^2 freshly cleaved pieces of mica for a deposition time of 35 min After that, mica was rinsed three times with 100 μl of the corresponding ionic aqueous solution The process of vesicle formation and deposition for the rest of the phospholipid bilayers used in this work's DLPC and DPPC (all of them from Sigma >98%) is the same as the one described for DMPC. In the case of DPPC, however, the temperature cycles for resuspension were set to ~50°C due to the higher T_M for this phospholipid

DSC measurements

Differential scanning calorimetry (DSC) measurements were performed with a MicroCal MC-2 (MicroCal, Northhampton, MA) The heating and cooling rate was usually 10°C h^{-1}, and the measurements were performed in the temperature interval from 10°C to 55°C. The reproducibility of the DSC experiments was checked by three consecutive scans of each sample

Temperature-controlled AFM imaging

AFM images were acquired with a Multimode (Digital Instruments, Santa Barbara, CA) microscope equipped with a J-Scanner AS 130V with fluid heat exchanger controlled by a Nanoscope IV electronics (Digital Instruments) in contact mode using V-shaped Si_3N_4 tips (OMCL TR400PSA, Olympus, Tokyo, Japan) cantilevers The applied force when obtaining topographic images was controlled by acquiring force plots before and after every image was captured so as to measure the force increment from the set point value Temperature controlled experiments were performed with a temperature controller stage (high temperature heater controller range up to 250°C, resolution 0 1°C, accuracy· 3%, temperature drift ±0 25°C, Digital Instruments) Basically, the temperature setup consists of a resistor placed between the scanner and the sample that transmits the heat to the sample from underneath The piezo is always kept under its Curie temperature by a cooler fluid circuit This applied temperature is the temperature that the heater displays as the "sample temperature" and the temperature that indeed has been used in most of the AFM-controlled studies

as the sample temperature. However, in conventional AFM imaging in a liquid environment, the mica sample is glued to a thin Teflon disk that is glued to a metallic holder. The whole sample remains attached to the microscope scanner by a magnet. Although the distance between the heating element and the sample itself (inside the buffer droplet) is typically <3–4 mm, the temperature gradient between the displayed and the real temperature is substantial (Fig. S1 in the Supplementary Material) and varies (up to ~25% at high temperatures) for different Teflon holders that differ only 1 mm in height. Therefore, calibration of individual sample holders becomes compulsory. Sample temperature is measured by a thermocouple (Cole Palmer (Vernon Hills, IL) thermocouple thermometer EW-91100-20 Digi Sense; resolution: 0.1C, accuracy: ±0.25% provided with Omega (Brattleboro, VT) precision fine wire thermocouples) that measures the temperature inside the buffer droplet just in contact with the sample surface. Upon imaging, temperature was varied from 16°C up to 85°C with a 0.5°C/min ramp. Before every image was acquired, a dwell time of 4–5 min lapsed to let the system equilibrate temperature. However, temperature equilibration was measured to be typically <45 s.

Force spectroscopy

Force spectroscopy was performed with the same setup using the force-extension mode. Force plots were acquired using V-shaped Si_3N_4 tips (OMCL TR400PSA, Olympus) with a nominal spring constant of 0.08 N/m when performing force curves on DLPC and DMPC and V-shaped Si_3N_4 tips (tip "F", Thermomicroscope, Sunnyvale, CA) with a nominal spring constant of 0.5 N/m when performing force plots on DPPC (higher yield threshold values (1)). Individual spring constants were calibrated using the equipartition theorem (thermal noise) (42) after having correctly measured the piezo sensitivity (V/nm) by measuring it at high voltages after several minutes of performing force plots to avoid hysteresis. It has to be pointed out that the results here shown within the same experiment were obtained with the same cantilever keeping the spot laser at the same position on the lever to avoid changes in the spring constant calculation (43). However, results have low scattering when using different tips and different samples (within 10% error). Tip radius was individually measured by imaging a silicon grating (MikroMasch (Tallinn, Estonia), Ultrasharp TGG01, silicon oxide 3 μm pitches). Individual radii were found to be 30 ± 10 nm, although little variation <20% was found for tips from the same wafer; ~300 curves were obtained for each temperature. All experiments were performed at the same indenting velocity (1 μm/s) so that the small effect of the velocity on the breakthrough force could be totally neglected. Applied forces, F, are given by $F = k_c \times \Delta$, where Δ is the cantilever deflection and k_c is the cantilever spring constant. The surface deformation is given as penetration (δ) evaluated as $\delta = z - \Delta$, where z represents the piezo-scanner displacement. X-, Y-, Z- piezo motion was calibrated with a Digital Instruments silicon oxide grid (STR10-1800P), 180 nm deep, 10 μm pitch.

RESULTS

Topographic evolution of a supported DMPC bilayer with temperature

Liposome deposition onto hydrophilic, negatively charged surfaces such as mica has been proved to be electrostatically governed: high ionic strength solutions give rise to compact, huge planar bilayers extending some micrometers, whereas under distilled water small discontinuous islands are formed (1). This is the main reason we have chosen to mainly work under high ionic strength conditions, since under these conditions the huge, completely formed bilayers allow us to follow the topography changes as the temperature is varied in a reproducible way. The evolution of the topography of a

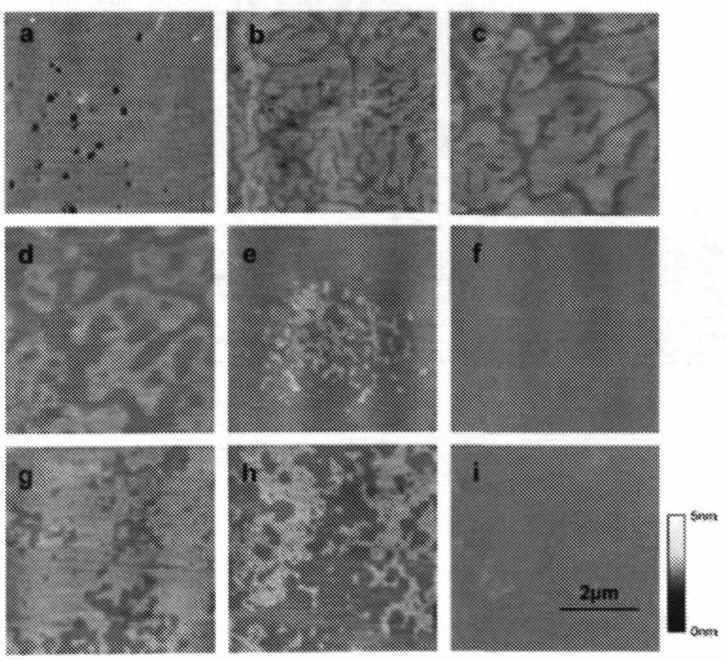

FIGURE 1 AFM contact mode images showing the phase transition for a DMPC-supported bilayer upon heating the sample (*a*) 19.0°C, (*b*) 24.4°C, (*c*) 27.2°C, (*d*) 28.3°C, (*e*) 29.3°C, (*f*) 30.3°C, (*g*) 31.3°C, (*h*) 32.9°C, and (*i*) 37.5°C. All images were acquired by applying a constant force of 1.5–2 nN.

DMPC bilayer from room temperature to 50°C is shown in Fig. 1 upon 5 × 5 μm^2 contact mode AFM images under high ionic strength conditions, which yield well-defined supported lipid single bilayers (1). At 19°C (Fig. 1 *a*) the gel phase (L_β) is observed. The black holes (defects in the bilayer) correspond to the mica support. From cross sections (see Fig. 2) the width of the bilayer can be measured to be 5 ± 0.3 nm, which corresponds to the height of a single supported bilayer (the fully hydrated DMPC bilayer is found to measure 5.99 nm at 10°C (44)). When increasing temperature up to 22°C (in all cases the registered temperature is the "real" temperature, lower than the temperature externally applied to the system, see the Materials and Methods section) ruptures on the extended L_β phase are observed. The initial temperature at which the first hint of phase transition is observed is in good accordance with the DSC main transition temperature peak (23.6°C, Fig. 2). Those lines, 0.5 ± 0.1 nm lower than the L_β surface, become wider as the temperature is increased, thus showing clear phase separation (Fig. 1 *b*, T = 24.4°C). The high domain corresponds to the remaining L_β phase and the low domain to the fluid-like L_α phase. Further increasing the temperature leads to an increased progressive disappearance of the L_β phase (Fig. 1 *c*, T = 27.2°C; Fig. 1 *d*, T = 28.3°C) until the whole surface is covered by the fluid-like phase (Fig. 1 *f*, T = 30.3 C). Therefore, the whole main transition is observed within ~5.5°C. The broader T_M width observed upon supported bilayers related to that observed in unilamellar vesicles in solution through DSC experiments might be due to the single bilayer nature of the SPB and to the substrate effect (23). Interestingly, upon further increasing temperature a new phase separation is observed (Fig. 1 *g*, T = 31.3°C). These two different phases have a difference of 0.6 ± 0.1 nm in height. The total height with respect to the mica surface cannot be assessed due to the lack of defects. The temperature gap that comprises the whole disappearance of the upper L_α phase ranges from 32.9°C (Fig. 1 *h*) to 37.5°C (Fig. 1 *i*). At higher temperatures (up to 80°C) no further topographic changes were observed. A complete sequence of evolution of the same scanned surface area is provided in the Supplementary Material (Fig. S12). Interestingly, the results concerning the evolution of the bilayer topography with temperature when measured under distilled water are basically the same as those observed under high ionic strength conditions. Nonetheless, under distilled water the phase transitions are not as clear as in the case of high ionic strength conditions because the islands are too small to assess a particular temperature the moment at which the transition starts. In any case, the temperature gap is still ~14°C to reach unambiguously the liquid phase upon raising the temperature. The first observed transition clearly corresponds to the gel phase-fluid phase ($L_\beta \rightarrow L_\alpha$) transition, and it is in perfect accordance with the main transition temperature peak observed upon DSC measurements. However, the nature of the second observed phase transition is unclear. Two possible explanations could account for the experimental observations. On the one hand, as stated in Leonenko et al. (23), this second transition could be associated with the formation of a fluid-disordered phase, perhaps with interdigitated or partially interdigitated lipid chains, but this new phase is not observed upon lipid bilayer extensive available literature or in our DSC measurements.

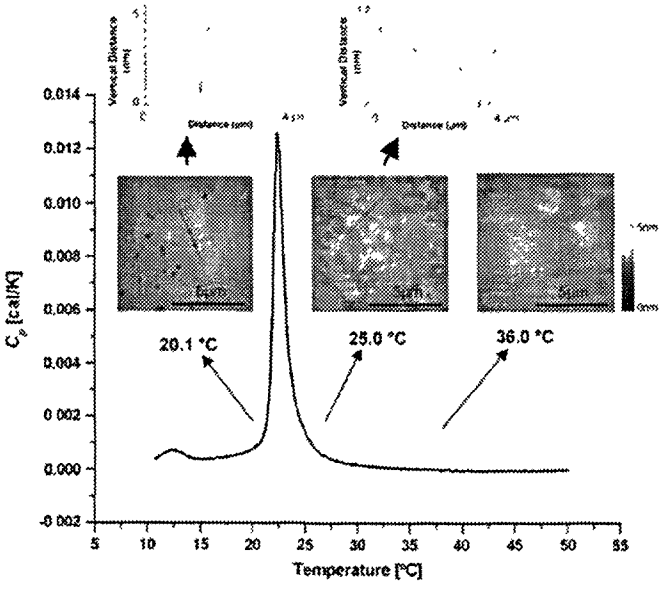

FIGURE 2 DSC register obtained in a DMPC unilamellar liposome solution under the same high ionic strength solution used upon AFM images and force spectroscopy experiments (150 mM NaCl + 20 mM MgCl$_2$, pH 7.4). The plot shows a peak centered at 23.6°C corresponding to the lipid main phase transition. In contrast, 10 × 10 μm^2 contact mode AFM images show the topography of the supported bilayer before (20.1°C) during (25°C), and after (36°C) the main phase transition. Although the main $L_\beta \rightarrow L_\alpha$ transition occurs within 3°C in solution, the temperature range broadens up to ~14°C when supported on mica.

On the other hand, the two observed transitions could belong to the same ($L_\beta \rightarrow L_\alpha$) transition after the decoupling of the phase behavior of the two leaflets of mica-supported PC bilayers as proposed upon the DSC results obtained on mica-supported bilayers (45) This finding would support the theory that the coupling between the two leaflets in a unique bilayer is weak (46) As it has been pointed out in Yang and Appleyard (45), the effect due to the substrate lipid interaction may be stronger than the interaction between leaflets, so the higher temperature transition would be due to the DMPC leaflet in contact with mica This behavior highlights the fact that the actual temperature at which the main phase temperature takes place is also highly sensitive to the environment surrounding the bilayer This possibility was excluded in Leonenko's et al (23) interpretation, since this would lead to more than two domains of different thickness at intermediate temperatures and instead only two domains at a time have been observed The only possibility is then that one leaflet melts completely before the other starts to melt Indeed, we do not exclude such possibility Further investigation involving Langmuir Blodgett monolayers may shed light on this issue I nally, a third interpretation concerning the possibility of having a multibilayer instead of a single bilayer deposited on the surface and therefore the two step gel fluid phase transition being associated to the presence of a first bilayer sticking on the mica support and the second transition being related to the second bilayer, less affected by this support, has been excluded Several reasons support this belief First, upon AFM images we realize that the depth between the bilayer surface (brighter regions) and the sub strate (darker regions) is ~4 5 nm, which is the depth of a single bilayer (also related to the width of the jump observed upon force spectroscopy measurements) Moreover, we can assess that there is not evidence of a first bilayer stacked on the surface since lateral force microscopy studies reveal the presence of a single bilayer deposited on the mica surface (47) Indeed, lateral force profiles show a clearly different behavior in the bilayer (also related with a discontinuity in the lateral force plot) and in the mica substrate Furthermore, the probability of having a double bilayer is much higher in PE membranes than in the case of PC membranes, where the deposition of a second PC bilayer on a first deposited bilayer is not favored (17) Therefore, for the reasons outlined above we tend to think that we only have a single bilayer deposited on the surface

In any case, it is clear that below 23°C only the solid like phase is present in the system, and above 37°C the whole surface is covered by the liquid-like phase These considerations have to be taken into account for further discussion in the forthcoming lines Finally, the evolution of the bilayer topography has been performed upon cooling the system from 45°C to ambient temperature The process appears to be reversible, since the phases observed during heating are recovered while cooling down to the initial temperature

Fig 2 shows a summary of the surface topography characteristics as a function of temperature before and after the main transition temperature The DSC thermogram has been acquired for unilamellar liposomes under the same high ionic strength solution used upon AFM imaging and force spectroscopy measurements, and it shows a main peak corresponding to the ($L_\beta \rightarrow L_\alpha$) transition at 23 6°C ± 1°C The same transition has been shown upon AFM images (Fig 1) to occur within a wide range of temperatures, namely, 23°C–37°C At temperatures below the main phase transition (20 1°C), the bilayer surface looks compact The small holes serve to measure the bilayer height (in this particular case, of 4 7 nm) Just after the main transition temperature (25 0°C), the phase has totally changed from the L_β phase into the L_α phase in solution, as can be seen from the DSC register, but two domains of different height Δh ~0 6 nm (cross section) are observed in supported bilayers The whole transition is over at 36°C, after the second transition has taken place Therefore, whereas the main transition takes place in solution within a temperature range of ~3°C (DSC register), the transition temperature range broadens up to ~14°C when phospholipids bilayers are surface supported Here it is worth pointing out that according to our data and also on account of the results available in the literature (48,49), increasing ionic strength gives rise to an increase in the T_M determination by DSC measurements in solution In our case this shift is ~0 3°C upon DSC measurements, but unfortunately this variation is difficult to assess when the bilayers stand supported on a substrate, especially due to the fact that under water, lipid bilayers do not form a continuous, huge bilayer as stressed above An in-depth molecular dynamics (MD) study concerning a finite number of phospholipid and water molecules dealing with the evolution of the interactions arising between them while varying the temperature would help us to understand the underlying processes from an atomistic point of view

Force spectroscopy on a supported DMPC bilayer

As above stated, lipid bilayers are shown to present a discontinuity in the force plot, this jump being related to the tip penetration into the bilayer The force at which this jump occurs is the maximum force that the membrane is able to withstand before the onset of plastic deformation occurs, and it is a reflection of the lateral forces that bind the phospholipid molecules together The question remains open, however, of whether it is only the solid (gel) phase that can be punctured with the AFM tip or if, in addition, the liquid phase also shows a jump in the force curve Since 1,2 dioleoyl 3 trimethylammonium-propane (DOTAP), (T_M = 0°C) (39,41), and 1,2 dioleoyl-*sn*-glycero 3 [phospho-L-serine] (DOPS), (T_M = −11°C) (38 39), bilayers have been punctured and we have recently observed jumps when indenting 1,2 dioleoyl *sn* glycero-3-phosphocholine (DOPC) (T_M = −20°C) and DLPC (T_M = −1°C) bilayers

(1), it seems clear that the liquid phase presents enough ordering and cohesion (jumps are related to molecular ordering (50)) to show the breakthrough. Then the real challenging point to be addressed is the evolution of the yield threshold force with temperature. To deal with this question we have formed a DMPC bilayer onto a freshly cleaved mica surface. A 200–300 μl buffered water droplet was deposited onto the sample, and the surface was imaged to check the presence of the bilayer. Continuous bilayer regions of ~40 μm were easily created after long deposition times (~35 min) in high ionic strength solutions. Once a good bilayer region was chosen, a set of 300 consecutive force plots over different places of the sample was performed. Interestingly, 80% of the force curves presented the jump which implies that bilayers self heal within the time of two successive force plots. In ~12–15% of the force plots, especially when conducted under high ionic strength conditions, a double jump in the force curve was observed. This second jump was interpreted as a lipid bilayer formed on the AFM tip (51) and was closely related to the presence of high ionic strength conditions. No relationship between the presence of such second jumps and temperatures has been observed. The recordings where two jumps have been observed have been excluded for data statistics. After having performed the force plots, the heater temperature was raised 5°C. Then, after waiting ~4–5 min for temperature equilibration, another set of 300 curves was performed. This process was repeated from ambient temperatures up to ~70°C–80°C. The setup was kept under high humidity conditions throughout the experiment. Fig. 3 shows four force curves obtained at different temperatures (*a*) 22°C, (*b*) 29.5°C, (*c*) 40.9°C, and (*d*) 52.4°C. The jump is clearly observed as a discontinuity in the force plot, and it occurs at ~11.0 nN (*a*), at ~5.5 nN in (*b*), at ~6.2 nN (*c*), and at ~5.8 nN (*d*). A statistical data treatment has been performed by fitting a Gaussian distribution to the histogram of the breakthrough forces obtained for each sampled temperature. The dotted line highlights the overall breakthrough force tendency as temperature is increased. Fig. 4 shows the evolution of the yield threshold

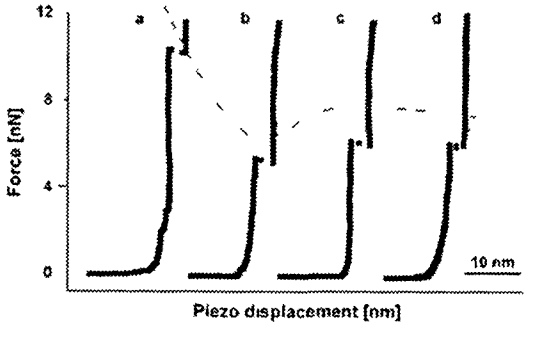

FIGURE 3 Force-distance curves obtained on a DMPC supported lipid bilayer at different temperatures (*a*) 20.1°C, (*b*) 29.5°C, (*c*) 40.9°C, and (*d*) 52.4°C. The discontinuity in the force-distance curve (breakthrough) indicates the tip penetration into the lipid bilayer, and the force at which it takes place is called yield threshold force. The dotted line highlights the overall breakthrough tendency as the temperature is increased.

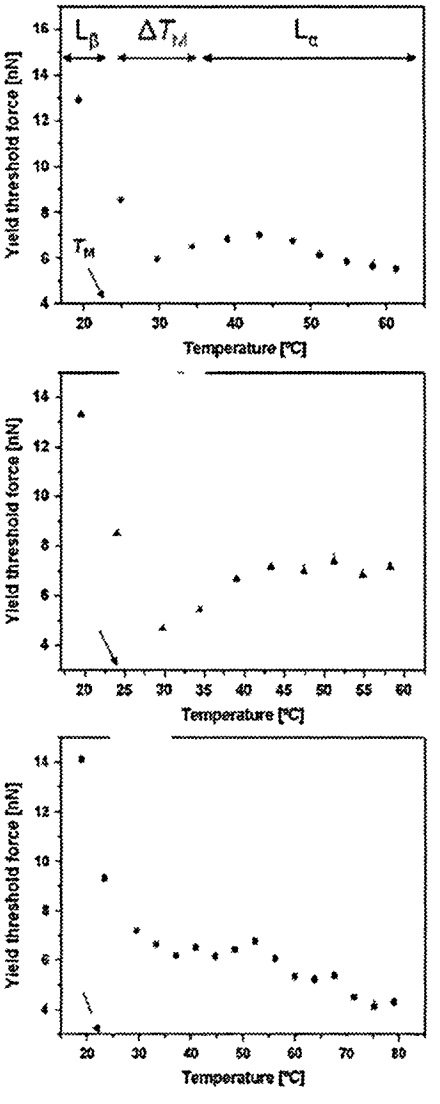

FIGURE 4 Yield threshold force dependence of a mica supported DMPC bilayer with temperature for three independent experiments (different tip–different sample). All measurements were performed under high ionic strength solution. Each point in the graph corresponds to the center value of a Gaussian fitting to the obtained histogram. Error bars stand for 1 standard deviation of the Gaussian fitting to the yield threshold force histograms. T_M stands for the main transition temperature obtained from DSC measurements. Dark arrows and for the temperature range (ΔT_M) in which phase transitions are observed in supported planar bilayers through AFM images (Fig. 1).

force for three independent experiments (different tip, different sample). Each point in the graph corresponds to the Gaussian center ± standard deviation. As can be observed, the yield threshold force occurs at ~13–15 nN for temperatures around 20°C. This is in accordance with the results obtained in García-Manyes et al. (1) for DMPC under high ionic strength (14.93 ± 0.09 nN). As temperature is increased, the yield threshold value occurs at lower force, and it reaches a minimum in force at ~25–33°C (~4.5–6 nN). This temperature range corresponds to the phase transitions observed in supported bilayers, as AFM images reveal (Fig. 1). Still, in every force plot the jump is observed, thus suggesting that even though the yield threshold force has sensibly decreased, the membrane has not lost its compactness. Further increasing temperature leads to an increase in the yield threshold force, up to ~7 nN. When temperature is further raised, it results in a more or less constant yield threshold force or even in a slight decrease in the breakthrough force, especially for temperatures >60°C. Therefore, the general picture of the process yields a high yield force value for temperatures below T_M and a sudden decrease in force at temperatures around T_M, thus creating a "well" in the plot around T_M. In each plot in Fig. 4 the dark area region corresponds to the temperature range in which the main transition phase has been observed upon contact images, thus highlighting the correspondence between the surface phase transition regime and the force well observed through force spectroscopy results. Upon rising temperature, the yield force rises again until a more or less stable value within the liquid-like phase.

DMPC is a good candidate to study its nanomechanical response within both solid-like and fluid-like phases and especially around the main transition temperature since its T_M value, 23°C, and its expanded range 23°C–36°C when bilayers are supported lies within ambient temperatures. Yet it does not allow studying the yield threshold evolution with temperature within the gel phase. To this aim we have performed the same experiment with DPPC, which only differs from DMPC in two more $-CH_2$ groups in both hydrophobic tails, which implies a higher T_M, ~41°C (45).

Topographic evolution of a DPPC bilayer with temperature

Fig. 5 shows the evolution of the surface topography with temperature. At room temperature (well below the T_M) (24.5°C, Fig. 5 *a*), the surface looks like the gel-phase observed for DMPC (Fig. 1 *a*). Many "holes" or defects can be observed, which allow us to measure the bilayer height (~5.1 nm). Those holes do not heal or disappear while continuously scanning the surface in contact mode at this temperature. However, as temperature is raised (Fig. 5 *b*, 37.7°C) the number of defects is greatly reduced until they completely disappear (Fig. 5 *c*, 38.7°C), thus implying a lateral expansion (increase in the area/lipid value) of the phospholipid molecules in the gel phase. At 44.8°C (Fig. 5 *d*)

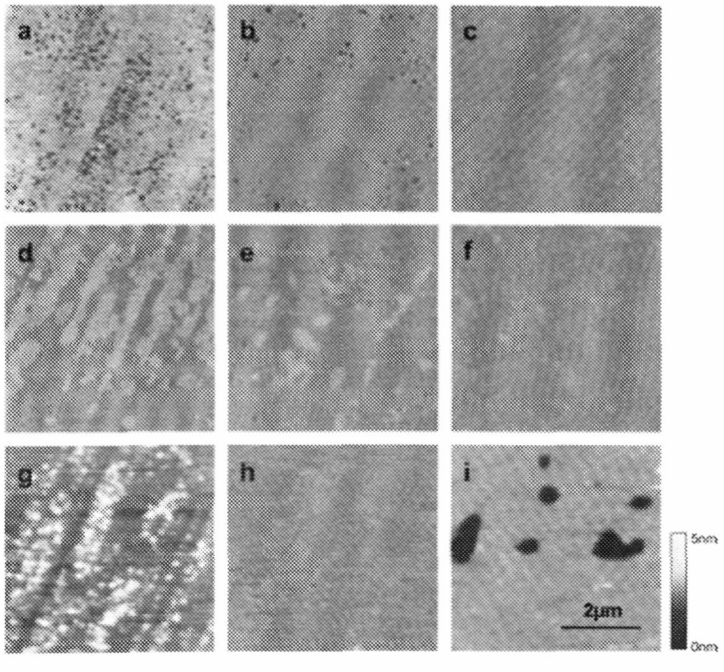

FIGURE 5 AFM contact mode images showing the main phase transition for a DPPC-supported bilayer upon heating the sample (*a*) 24.5°C, (*b*) 37.7°C, (*c*) 38.7°C, (*d*) 44.8°C, (*e*) 48.3°C, (*f*) 51.4°C, (*g*) 52.9°C, (*h*) 59.4°C, and cooling back to (*i*) 34.2°C.

the $L_{\beta'}$ phase starts to separate from the lower fluid like L_α phase This L_α phase expands as temperature is increased (Fig 5 e T 48 3°C) until the total disappearance of the $L_{\beta'}$ phase (Fig 5 f, T = 51 4°C) thus implying that the whole surface is covered by the fluid-like phase On further heating the sample, the liquid like phase is being disrupted (Fig 5 g 52 9°C) by the appearance of a lower phase, which expands and finally totally covers the surface (Fig 5 h, 59 4°C) Finally, upon cooling the system back to 34 2°C the surface recovers its compact, initial $L_{\beta'}$ phase (Fig 5 i). Interestingly the solid like phase obtained after a heating cooling process looks typically much more compact than the initial $L_{\beta'}$ phase, perhaps on account of the better rearrangement of phospholipids due to the temperature effect, in this case the number of defects or holes is typically smaller even though they are bigger than those observed in the initial $L_{\beta'}$ phase (Fig 5 a) Regarding the main phase transition, it occurs 44 8–51 5 C (first transition) and 52–59°C (second transition) Regardless of whether both are considered to be part of the $L_{\beta'} \rightarrow L_\alpha$ transition (separate temperature ranges for both bilayer leaflets) or the second transition being related to the formation of a fluid disordered phase it is clear that phase transition occurs in surface within a range of 15 C, i e, 45–60°C Overall, the observed process is in the case of DPPC very similar to that observed by Leonenko et al (23)

Force spectroscopy on a DPPC bilayer

Once the surface topographic characteristics and their dependence with temperature were well known, we performed a force spectroscopy experiment analogous to that performed with DMPC The evolution of the yield threshold force with temperature for two independent experiments is shown in Fig 6 At low temperature (~24°C) the yield threshold force was found to be ~ 23 26 nN, which is again in very good accordance with the results obtained in Garcia-Manyes et al (1) Here we have to outline the high force needed to penetrate a DPPC membrane in the solid like phase Note that this force is similar to the force needed to indent an alkali halide single crystal (35) thus highlighting the strong lateral interactions created between two ordered neighboring phospholipid molecules Indeed, force experiments on DPPC bilayers were performed with a stiffer cantilever (0 5 N/m) to reach the yield threshold force point On increasing temperature, still in the solid-like phase, we observe a decrease in the yield threshold force This decrease could be accounted for by the increase in the area/lipid value with temperature, which is in accordance with the surface mobility (defects disappearance) observations upon AFM images (Fig 5, *a* and *b*) Thus the higher the area per lipid value (less compact structure, reduced lateral interaction between neighboring molecules), the easier for the AFM tip to penetrate the bilayer The yield threshold force reaches its minimum (~5–7 nN) at ~46°C 50°C Further increasing temperature within the liquid like phase does not seriously affect the yield threshold force value It

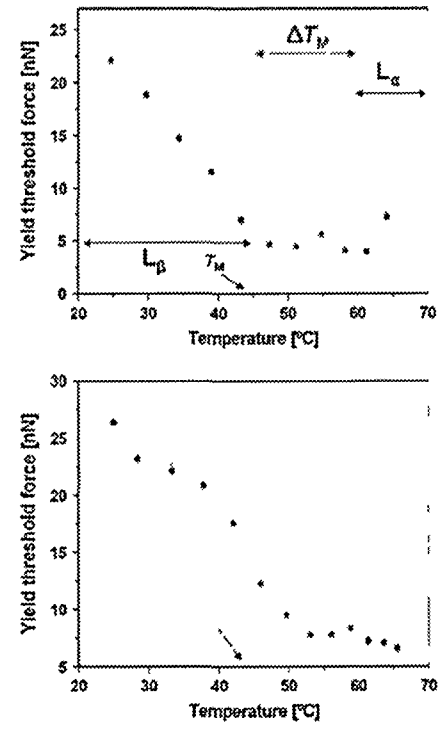

FIGURE 6 Yield threshold force dependence of a mica supported DPPC bilayer with temperature for two independent experiments (different tip different sample) All measurements were performed under buffer ionic strength solution Each point in the graph corresponds to the center value of a Gaussian fit ans to the obtained histogram Error bars stand for standard deviation of the Gaussian fit ans to the yield threshold force histograms T_M stands for the main transition temperature obtained from DSC measurements Dark areas stand for the temperature range (ΔT_M) in which phase transitions are observed in supported phenyl bilayers through AFM images (Fig 5)

varies around an average value of 6 nN Dark areas in Fig 6 account for the temperature range in which phase transition has been observed in mica supported DPPC bilayers thanks to AFM contact images In conclusion, we have observed that for DPPC supported bilayers i) solid like phase presents a higher mechanical stability than fluid-like phase (the yield threshold force being up to three fold greater in the $L_{\beta'}$ phase region than in the L_α region for temperatures 20 C below the main transition temperature) ii) within the solid like phase yield threshold value decreases with increasing temperature This process may be accounted for by the reduction in area/lipid value of the DPPC bilayer as temperature is increased, thus lowering lateral interaction between neighboring molecules and iii) the lower yield threshold values occur also for DPPC bilayers in the temperature range where phase transitions are taking place, yielding very similar results to those obtained for DMPC bilayers

Force spectroscopy on a DLPC bilayer

The two studied lipid bilayers have a high T_M, allowing us to make a quantitative comparison of the evolution of the yield threshold value between the gel and the liquid phase. To conclude with, we have studied the nanomechanical behavior of a DLPC bilayer, with a T_M value at a much lower temperature (−1°C). Therefore, we are dealing with the liquid phase at temperatures well above (20–60°C) T_M. Fig. 7 *a* shows a 5 × 5 μm^2 contact mode AFM image of the totally covered surface acquired at 25°C. Here again in >80% of the recordings, the jump in the force plot has been observed, despite the liquid nature of the bilayer. An example is shown in Fig. 7 *b*, where a force-distance curve for a DLPC bilayer is observed. The yield threshold is pointed with an arrow. The evolution of the yield threshold force with temperature for two independent experiments (different tips, different samples) is shown in Fig. 7, *c* and *d*. At 23°C the yield threshold is observed at ~9 nN. Increasing temperature yields to a decrease in the yield threshold force until reaching a minimum value at ~35°C (~5 nN). Surprisingly, at higher temperatures the yield threshold force started to increase until reaching maximum values at the higher sampled temperatures (~11–13 nN at 60–65°C). This unexpected, reproducible behavior is indeed difficult to interpret, although a possible explanation is discussed below.

A different effect of Ion binding on the nanomechanical response of the bilayer in the L_α and L_β phases

Up to this moment we have dealt with the evolution of the nanomechanics of supported lipid bilayers with temperature. All the experiments were performed under high ionic strength solutions (150 mM NaCl + 20 mM $MgCl_2$, pH ≈

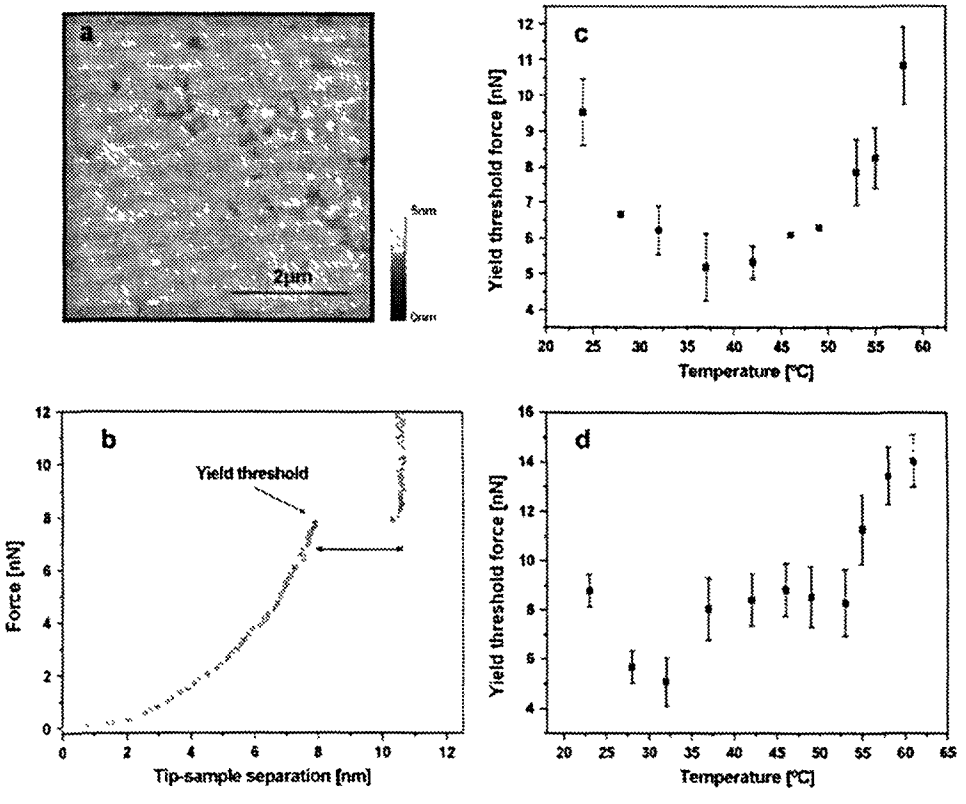

FIGURE 7 (*a*) 5 × 5 μm^2 contact mode AFM image of DLPC-supported bilayer showing total surface coverage. Force plots were performed in different positions all around the surface, yielding force-distance curves such as that observed in *b*, where the discontinuity in the curve is shown (yield threshold point) to and *d*) Yield threshold force dependence of a mica supported DLPC bilayer with temperature for two independent experiments (different tip, different sample). Each point in the graph corresponds to the center value of a Gaussian fitting to the obtained histogram. Error bars stand for standard deviation of the Gaussian fitting to the yield threshold force histograms. All measurements are performed in the liquid like phase, since T_M (−1 °C) is far below the sampled temperatures.

7.4), mainly because i), these experimental conditions mimic physiological conditions, and also because ii), ionic strength plays a key role upon bilayer deposition onto a mica surface (17). However, ionic strength (ion-binding effect) plays a key role in membrane nanomechanics. This fact has been recently observed through MD simulations (49,52–56) and also addressed by us in a recent work (1). However, most of these MD simulations were performed in the liquid-like phase for the studied phospholipid bilayers. We now have the chance of experimentally studying the role of ionic strength on both the solid-like and the liquid-like phases and to quantitatively compare the nanomechanical effect of cation binding within the two different phases for the same phospholipid molecule. Although the role of ionic strength has been previously addressed for the solid-like phase (1), showing a great increase of the yield threshold value as ionic strength was added to the measuring system, the effect of ion-binding on the nanomechanics of the system has not been studied in the fluid-like phase. Fig. 8 *a* shows the evolution of the yield threshold force with temperature for a DMPC-supported bilayer formed and measured under high ionic strength conditions (Fig. 8 *a*, *black circles*) and formed and measured in buffered water (*white circles*). Both experiments were conducted with the same tip. Although the trend is similar for both curves (both showing the well), the curve obtained for the bilayer measured in water is clearly shifted to lower force values, thus indicating that ionic strength has an effect on both the solid and the liquid phases. However, the yield threshold force difference within the solid phase (*vertical left arrow*) is much higher (ΔF_y = ~9 nN) than the difference found within the liquid phase (ΔF_y = ~3 nN), (*vertical right arrow*). Similar results were found when comparing the yield threshold force evolution for a DPPC bilayer (Fig. 8 *b*) when it was formed and measured under higher strength conditions (*black circles*) and in distilled water (*white circles*). Within the solid-like phase (*vertical left arrow*), the yield threshold force difference appears to be quite constant within the temperature range 22°C–42°C (ΔF_y = ~13–15 nN) and higher than the observed difference within the liquid-like phase (ΔF_y = ~1.5–2.5 nN). Therefore, we come to the conclusion that, even though ion binding seems to an have effect both in the liquid and gel phase, it is in the gel phase where its role is enhanced the most.

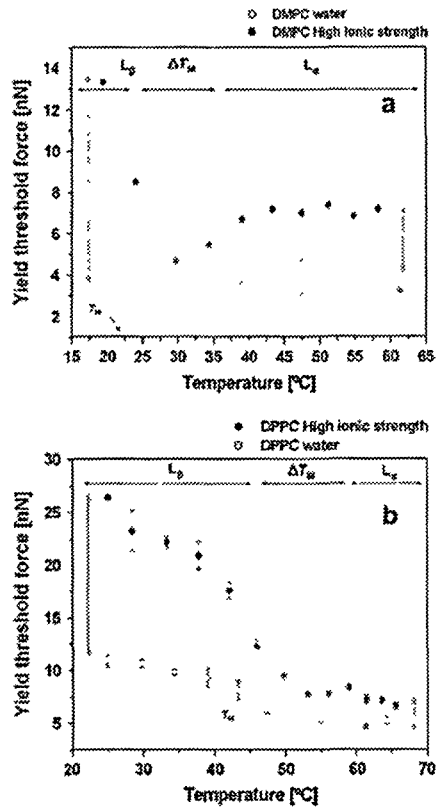

FIGURE 8 Yield threshold force dependence with temperature of a mica-supported (*a*) DMPC bilayer and (*b*) DPPC bilayer formed and measured in buffered distilled water (*white circles*) and in buffered high ionic strength solution (*black circles*). In both cases both curves exhibit a well around the surface transition temperature ΔT_m (*dashed region*) and the bilayer measured under high ionic strength conditions is shifted to higher yield force values, thus suggesting a higher stiffness, both in the solid-like and in the liquid-like phases. The difference in the yield threshold force is enhanced in the solid-state phase (*left arrow*) with respect to the liquid-like phase (*right arrow*). Both curves (under high ionic strength and distilled water) for DMPC and DPPC were performed with the same tip (k_c = 0.08 N/m for DMPC and k_c = 0.5 N/m for DPPC).

DISCUSSION

A full interpretation of the obtained results is not straightforward. A first qualitative approach could be made in terms of A (area per molecule) values. Indeed, the A values are known to be smaller (more packed structures) for the gel phase than for the liquid-like phase. Therefore, whereas A = 47.2 ± 0.5 Å^2 for fully hydrated DMPC bilayers at 10°C (gel phase) (44), it turns out to be A = 60.6 ± 0.5 Å^2 for fully hydrated fluid phase at 30°C (57), resulting in a reduction of the 22% in the gel phase with respect to the liquid phase. A similar trend is observed for DPPC bilayers, yielding A = 47.9 Å^2 for the gel phase (20°C) and A = 64 Å^2 for the fluid phase (50°C) (2). A more packed structure results in an increase of the order parameter and to an enhancement of lateral interactions between neighboring groups. As a consequence, the observed experimental trend (a higher resistance of the whole phospholipids network upon breakthrough in the gel phase and a decrease of the yield threshold value in the liquid phase) is in good accordance with area per lipid values considerations. This simple interpretation can qualitatively explain both the difference in yield threshold value between

the solid phase and the liquid phase for a given phospholipid (DMPC and DPPC) and also within the solid phase (in the case of DPPC) Nonetheless, there are two features in the yield threshold force versus temperature plots that cannot be explained only in terms of increasing the lateral area per lipid values from the gel phase to the fluid phase On the one hand, the graphs corresponding to DMPC (Fig 4) and to DPPC (Fig 6) show a minimum in the yield threshold force at temperatures close to their T_M On the other hand, and especially in the case of DLPC (Fig 7), the yield threshold value increases at high temperatures ($T > 50°C$ in the case of DLPC) after a deep well

Concerning the first issue, it is clear that the membrane is easier to be punctured (i e , becomes "softer", the breakthrough event occurs at lower forces) at temperatures close to the main transition temperature, resulting in a well in the graph Therefore, it could also be considered that around the T_M, the membrane exhibits an "anomalous" softening mechanical behavior In fact, many physical quantities have been found to display an anomalous behavior around T_M, such as heat capacitance, ζ-potential (4), electric conductivity (5), Na^+ permeability (6), NMR order parameter (7), or swelling (8) The latter is especially interesting since it has been reported by various groups and is directly related to structural and mechanical characteristics The experimental observation that with decreasing temperature, fluid-like, L_α, DMPC and DPPC bilayers exhibit a nonlinear increase in their lamellar repeat spacing, d, of 3–5 Å, is known as "anomalous swelling" (58) The origin of such swelling has been a matter of scientific discussion for years, although the most recent contributions tend to assess that it is the expansion of the water layer (d_w) rather than an expansion of the hydrophilic phosphatidylcholine headgroup or an anomalous expansion of the hydrophobic tail, the last responsible for this unexpected thickness increase (8) After excluding the possibility that the anomalous expansion of d_w could be attributed to changes in either the hydration or the van der Waals force, Pabst and co-workers (8) came to the conclusion through the measurement of the Caille fluctuation parameter (η_1) in multilamellar vesicles that the expansion of d_w is due to steric repulsion of bilayers caused by increased fluctuations Similar conclusions were reached upon NMR ^2H measurements, which have shown an "anomalous disordering" of the interbilayer water around the main phase transition (7,59) These observations, together with osmotic pressure studies, conclude that bilayers soften in the vicinity of T_M, experiencing increased levels of repulsion Overall, these anomalies strongly suggest that lipid bilayers undergo a significant structural rearrangement in the headgroup and in the acyl chain regions around the main transition Interbilayer water and hydration processes seem to play a key role upon membrane structural stability and seem to be strongly correlated to the ordering in the headgroups as electron spin resonance experiments confirm (9) Indeed, recent MD simulation results demonstrate than 76% of DMPC molecules in the bilayer are linked by single or multiple water bridges (60) and that DMPC headgroups also interact directly via Coulombic interaction between negatively charged phosphate or carbonyl oxygen atoms of another molecule Those two short-range interactions present in the liquid crystalline phase give rise to long-lived clusters that form an extended network of interactions among PC groups (61) These interactions link 98% of all PC molecules in the membrane, thus highlighting the role of PC headgroup-headgroup interactions in the stability of the membrane Besides, the presence of cations within the headgroup network is likely to enhance even more such interactions between neighboring headgroups (49,52,61) In any case, and even in the absence of salt, for the reasons outlined above, it seems clear that water plays a key role in membrane stability Besides ^2H NMR measurements (that pointed out the reduction in interbilayer water ordering at the main phase transition and interpreted this fact in terms of a coupling between fluctuations in interbilayer water concentration and lateral density fluctuations in the headgroup region), ESR measurements show that ordering of the headgroups and ordering of the interbilayer water are correlated (which is consistent with the membrane picture revealed by MD simulations) Furthermore, these results suggest that both ordering of the headgroups and of the interbilayer water are inversely correlated with the degree of hydration of lipid bilayers At T_M, the ordering of headgroups and the ordering of interbilayer water are the lowest, and the swelling of the bilayers reaches their maximum by increasing hydration of headgroups near the main phase transition, taking into account that dehydration or hydration of bilayers is a dynamic process of water moving between the interbilayer region and the bulk water phase This result is consistent with the decrease in the yield threshold force observed upon ethanol addition to the measuring solution (1) that is known to decrease interbilayer water ordering (62)

Besides interbilayer water and hydration of the polar groups several studies have been conducted regarding the structure of the hydrocarbon chains of phospholipid bilayers around T_M and its effect on the mechanical behavior of PC bilayers (63,64) More precisely, measurements of properties such as bending rigidity (K_c) (8) have concluded that a softening of the bilayer takes place around T_M (65) Lee et al (66) detected a decrease in K_c studying DPPC vesicles at variable temperatures by means of optical methods around DPPC transition temperature This fact had been previously reported by Heimburg et al (67) by using Monte Carlo simulations to study the mechanics of DPPC bilayers This K_c variation was attributed to a hydrocarbon chain melting around T_M Previous works performed by Needham and Evans (68,69) on the mechanics of giant vesicles suspended on glass micropipettes highlighted the key role of hydrocarbon-chain disorder in the DMPC vesicles transition process They found an increase of the surface shear viscosity while decreasing temperature from liquid phase through T_M until

reaching gel phase, showing the softening of the bilayer around T_M. Measurements of the widths of the bilayers in different phases led us to conclude that there is some degree of rotameric chain disorder as the bilayer approaches its T_M. This panorama borne in mind, it seems quite clear that around the T_M hydrocarbon chain, headgroup and interbilayer water, a key element upon membrane stability, present the lowest ordering, which is again increased at lower and upper temperatures. Around T_M thus, the AFM tip can penetrate the bilayer easier, and this is reflected in the lower yield threshold force observed in Figs. 4 and 6.

The second striking experimental observation is that the yield threshold force increases at high temperatures ($T >$ 50°C) for DLPC. Of course, in the whole range of temperatures, DLPC is in the L_α phase. Therefore, due to the enhancement of steric fluctuations and the increase of the lateral area/lipid value with temperature, one would expect a decrease of the yield threshold force with temperature. This trend is accomplished for temperatures 20–45°C. However, as temperature is further increased, the yield threshold force increases. This experimental feature has been observed for >10 individual temperature ramp series using different samples and different tips, and the obtained results have been always reproducible. This experimental trend is presently lacking interpretation. There is, however, an extra parameter that could (partially) account for this fact. Although the thickness of the interbilayer water increases with temperature the membrane thickness, d_B, decreases with temperature (8,70). Therefore the absolute value of the linear thermal expansion coefficient, α, decreases linearly at high temperatures (from 70°C to 40°C in the case of 1-palmitoyl-2-oleoyl-*sn*-glycero-3-phosphocholine (POPC)), indicating reduced bilayer elasticity (70). In this case, then, the reduced hydrocarbon chain elasticity term (higher bilayer stiffness) would dominate over the entropic fluctuation term at temperatures far above T_M, and it would be, therefore, the hydrophobic chain that is mainly responsible for membrane stability rather than the less-ordered headgroup moiety. Additional future work on this particular issue may help to shed light onto this question.

Regarding the role of ions upon membrane stability, recent MD simulation results have demonstrated (49,52,53) that the presence of cations (such as in the results presented here, namely, Na^+ and Ca^{2+}) in the phospholipids network would change drastically the structural and dynamical properties of the PC membranes. On average, every Na^+ cation binds to three carbonyl oxygens and to 1–2 water oxygens. Due to their threefold increased size as compared to single lipids, these complexes are less mobile. As a consequence, a decrease in the average area per lipid from 0.655 nm^2 to 0.606 nm^2 (>8%) is observed for POPC when Na^+ cations are introduced in the system, giving rise to a more compact overall structure. Indeed, the difference in the area per group is also reflected by the ordering of the lipid hydrocarbon tails (49,53). A similar case applied to Ca^{2+}, each Ca^{2+} cation binding to 4.2 PC heads on average. Therefore, and according to those MD simulations, the higher order structure promoted by ions on the bilayer, which give rise to a reduction in average area per lipid (higher compactness) and to a more rigid structure (lower diffusion coefficient), may be the cause for the higher membrane stability experimentally observed through the nanomechanical response of the system obtained by force spectroscopy measurements (1). In this work, we extend these results, mainly performed on the gel phase, to the liquid-like phase, and we confirm that indeed ion binding gives rise to a higher yield threshold force value within the whole range of sampled temperatures. However, the increase in yield threshold force due to the presence of ions in the measuring solution is much more evident in the gel phase than in the liquid-like phase, probably due to the lower distance between the neighboring phospholipid molecules forming the bilayer in the gel phase, which allows cations to enhance even more lateral interactions between neighboring molecules.

CONCLUSIONS

The effect of temperature on the nanomechanical properties of supported lipid bilayers has been experimentally studied by force spectroscopy in a quantitative way. We have related the evolution of the force required to penetrate the bilayer with an AFM tip (which is a direct measure of bilayer compactness) with the structural phase transitions observed upon AFM contact images. The main phase transition ($L_\beta \rightarrow L_\alpha$) takes place in supported bilayers within a range of temperatures of ~10–13°C. Phase transitions have indeed a clear mechanical effect on the stability of the bilayer. As expected, the solid-like phase shows a much higher resistance upon breakthrough than the fluid-like phase as proved for DMPC- and DPPC supported bilayers. Besides, although temperature has a strong effect on the nanomechanics of the solid-like phase, it does not have such a huge impact on the yield threshold value in the liquid-like phase, at least for a temperature range of 10–60°C above T_M. Interestingly, the yield force versus temperature plot shows a well for temperatures around T_M (in close relationship with AFM images), and hence an anomalous mechanical softening behavior has been assessed. This unexpected behavior around T_M has also been widely reported for many physical quantities, thus indicating that the membrane undergoes important structural changes within this temperature range. The interpretation of the nanomechanical response of the system within this temperature range has been performed in light of the new available data provided with MD simulations, which outline the role of water upon membrane mechanical stability and also according to data provided with other experimental techniques, mainly performed with multilamellar systems and we are now relating them to single supported bilayers. Our results experimentally corroborate the predictions that the membrane softens around

T_M on account of enhanced steric repulsions because of the decrease in headgroup ordering and also because of the disorder induced in the hydrocarbon chains in the vicinity of T_M. The anomalous trend observed for DLPC at high temperatures still lacks full interpretation, although the increase of bilayer stiffness at high temperatures could partially account for the observed experimental results.

Last but not least, the role of ion binding upon membrane stability within the two different phases has also been discussed, suggesting that although ion binding increases the yield threshold force within all ranges of temperature (and different phases), it is in the gel phase where this effect is more outstanding. Summarizing, this work shows how temperature-governed structural processes can have a mechanical response at the nanometer/nanonewton scale and how phase transitions have mechanical implications. It also highlights the use of temperature-controlled AFM for the study of biologically relevant tissues that are temperature dependent at the nanometer scale.

SUPPLEMENTARY MATERIAL

An online supplement to this article can be found by visiting BJ Online at http://www.biophysj.org.

We thank Dr. Jordi Hernandez-Borrell (UB) and Dr. Antoni Morros (UAB) for kindly allowing us to use the DSC equipment and also Òscar Domenech for helpful discussions.

S. G. M. thanks Departament d'Universitats, Recerca i Societat de la Informacio (DURSI) (Generalitat de Catalunya) for a grant and we all thank DURSI (Generalitat de Catalunya) for financial support through projects 2000SGR017 and AGP99-10.

REFERENCES

1. Garcia-Manyes, S., G. Oncins, and F. Sanz. 2005. Effect of ion-binding and chemical phospholipid structure on the nanomechanics of lipid bilayers studied by force spectroscopy. *Biophys. J.* 89:1812–1826.

2. Nagle, J. F., and S. Tristram-Nagle. 2000. Structure of lipid bilayers. *Biochim. Biophys. Acta.* 1469:159–195.

3. Nagle, J. F., H. I. Petrache, N. Gouliaev, S. Tristram-Nagle, Y. F. Liu, R. M. Suter, and K. Gawrisch. 1998. Multiple mechanisms for critical behavior in the biologically relevant phase of lecithin bilayers. *Phys. Rev.* 58:7769–7776.

4. Makino, K., T. Yamada, M. Kimura, T. Oka, H. Ohshima, and T. Kondo. 1991. Temperature- and ionic strength-induced conformational changes in the lipid head-group region of liposomes as suggested by zeta potential data. *Biophys. Chem.* 41:175–183.

5. Wu, S. H.-W., and H. M. McConnel. 1973. Lateral phase separations and perpendicular transport in membranes. *Biochem. Biophys. Res. Commun.* 55:484–491.

6. Papahadjopoulos, D., K. Jacobson, S. Nir, and T. Isac. 1973. Phase transitions in phospholipid vesicles. Fluorescence polarization and permeability measurements concerning the effect of temperature and cholesterol. *Biochim. Biophys. Acta.* 311:330–348.

7. Pope, J. M., L. Walker, B. A. Cornell, and G. W. Francis. 1981. NMR study of synthetic lecithin bilayers in the vicinity of the gel-liquid-crystal transition. *Biophys. J.* 35:509–520.

8. Pabst, G., J. Katsaras, V. A. Raghunathan, and M. Rappolt. 2003. Structure and interactions in the anomalous swelling regime of phospholipid bilayers. *Langmuir.* 19:1716–1722.

9. Ge, M., and J. H. Freed. 2003. Hydration structure, and molecular interactions in the headgroup region of dioleoylphosphatidylcholine bilayers: an electron spin resonance study. *Biophys. J.* 85:4023–4040.

10. Leonenko, Z. V., A. Carnini, and D. T. Cramb. 2000. Supported planar bilayer formation by vesicle fusion: the interaction of phospholipid vesicles with surfaces and the effect of gramicidin on bilayer properties using atomic force microscopy. *Biochim. Biophys. Acta.* 1509:131–147.

11. Jass, J., T. Tjarnhage, and G. Puu. 2000. From liposomes to supported, planar bilayer structures on hydrophilic and hydrophobic surfaces: an atomic force microscopy study. *Biophys. J.* 79:3153–3163.

12. Sackmann, E. 1996. Supported membranes: scientific and practical applications. *Science.* 271:43–48.

13. Benz, M., T. Gutsmann, N. Chen, R. Tadmor, and J. Israelachvili. 2004. Correlation of AFM and SFA measurements concerning the stability of supported lipid bilayers. *Biophys. J.* 86:870–879.

14. Kaasgaard, T., C. Leidy, J. H. Ipsen, O. G. Mouritsen, and K. Jorgensen. 2001. In situ atomic force microscope imaging of supported lipid bilayers. *Single Molecules.* 2:105–108.

15. Schneider, J., Y. F. Dufrene, W. R. Barger Jr., and G. U. Lee. 2000. Atomic force microscope image contrast mechanisms on supported lipid bilayers. *Biophys. J.* 79:1107–1118.

16. Schneider, J., W. Barger, and G. U. Lee. 2003. Nanometer scale surface properties of supported lipid bilayers measured with hydrophobic and hydrophilic atomic force microscope probes. *Langmuir.* 19:1899–1907.

17. Egawa, H., and K. Furusawa. 1999. Liposome adhesion on mica surface studied by atomic force microscopy. *Langmuir.* 15:1660–1666.

18. Silin, V. I., H. Wieder, J. T. Woodward, G. Valincius, A. Offenhausser, and A. L. Plant. 2002. The role of surface free energy on the formation of hybrid bilayer membranes. *J. Am. Chem. Soc.* 124:14676–14683.

19. Zasadzinski, J. A. N., C. A. Helm, M. L. Longo, A. L. Weisenhorn, S. A. C. Gould, and P. K. Hansma. 1991. Atomic force microscopy of hydrated phosphatidylethanolamine bilayers. *Biophys. J.* 59:755–760.

20. Egger, M., F. Ohnesorge, A. L. Weisenhorn, S. P. Heyn, B. Drake, C. B. Prater, S. A. C. Gould, P. K. Hansma, and H. E. Gaub. 1990. Wet lipid-protein membranes imaged at submolecular resolution by atomic force microscopy. *J. Struct. Biol.* 103:89–94.

21. Hansma, H. G., A. L. Weisenhorn, A. B. Edmundson, H. E. Gaub, and P. K. Hansma. 1991. Atomic force microscopy—seeing molecules of lipid and immunoglobulin. *Clin. Chem.* 37:1497–1501.

22. Butt, H. J., E. K. Wolff, S. A. C. Gould, B. D. Northern, C. M. Peterson, and P. K. Hansma. 1990. Imaging cells with the atomic force microscope. *J. Struct. Biol.* 105:54–61.

23. Leonenko, Z. V., E. Finot, H. Ma, T. E. Dahms, and D. T. Cramb. 2004. Investigation of temperature-induced phase transitions in DOPC and DPPC phospholipid bilayers using temperature-controlled scanning force microscopy. *Biophys. J.* 86:3783–3793.

24. Giocondi, M. C., and C. Le Grimellec. 2004. Temperature dependence of the surface topography in dimyristoylphosphatidylcholine/distearoylphosphatidylcholine multibilayers. *Biophys. J.* 86:2218–2230.

25. Enders, O., A. Ngezahayo, M. Wiechmann, F. Leisten, and H. A. Kolb. 2004. Structural calorimetry of main transition of supported DMPC bilayers by temperature-controlled AFM. *Biophys. J.* 87:2522–2531.

26. Seantier, B., C. Breffa, O. Felix, and G. Decher. 2004. In situ investigations of the formation of mixed supported lipid bilayers close to the phase transition temperature. *Nano Lett.* 4:5–10.

27. Tokumasu, F., A. J. Jin, and J. A. Dvorak. 2002. Lipid membrane phase behaviour elucidated in real time by controlled environment atomic force microscopy. *J. Electron Microsc. (Tokyo).* 51:1–9.

28. Giocondi, M. C., L. Pacheco, P. E. Milhiet, and C. Le Grimellec. 2001. Temperature dependence of the topology of supported dimyristoyl distearoyl phosphatidylcholine bilayers. *Ultramicroscopy.* 86:151–157.

29 Weisenhorn, A L, P Maivald, H J Butt, and P K Hansma 1992 Measuring adhesion attraction, and repulsion between surfaces in liquids with an atomic-force microscope *Phys Rev B* 45 11226–11232

30 Jaschke, M, H J Butt H E Gtub, and S Manne 1997 Surfactant aggregates at a metal surface *Langmuir* 13 1381–1384

31 O Shea, S J, and M E Welland 1998 Atomic force microscopy at solid liquid interfaces *Langmuir* 14 4186–4197

32 Oshea, S J, M E Welland and T Rayment 1992 Solvation forces near a graphite surface measured with an atomic force microscope *Appl Phys Lett* 60 2356–2358

33 Franz, V, and H J Butt 2002 Confined liquids solvation forces in liquid alcohols between solid surfaces *J Phys Chem B* 106 1703–1708

34 Sun, G X, E Bonaccurso V Franz, and H J Butt 2002 Confined liquid simultaneous observation of a molecularly layered structure and hydrodynamic slip *J Chem Phys* 117 10311–10314

35 Fraxedas J, S Garcia Manyes P Gorostiza, and F Sanz 2002 Nanoindentation toward the sensing of atomic interactions *Proc Natl Acad Sci USA* 99 5228–5232

36 Dufrene, Y F, T Boland J W Schneider, W R Barger, and G U Lee 1998 Characterization of the physical properties of model biomembranes at the nanometer scale with the atomic force microscope *Faraday Discuss* 111 79–94

37 Richter, R P, and A Brisson 2003 Characterization of lipid bilayers and protein assemblies supported on rough surfaces by atomic force microscopy *Langmuir* 19 1632–1640

38 Franz V, S Loi, H Muller, E Bamberg and H J Butt 2002 Tip penetration through lipid bilayers in atomic force microscopy *Colloids Surf B Biointerfaces* 23 191–200

39 Loi, S, G Sun V Franz, and H J Butt 2002 Rupture of molecular thin films observed in atomic force microscopy II Experiment *Phys Rev* 66 031602

40 Butt, H J, and V Franz 2002 Rupture of molecular thin films observed in atomic force microscopy I Theory *Phys Rev* 66 031601

41 Mueller H, H J Butt and E Bamberg 2000 Adsorption of membrane-associated proteins to lipid bilayers studied with an atomic force microscope myelin basic protein and cytochrome c *J Phys Chem B* 104 4552–4559

42 Florin, E L, M Rief, H Lehmann, M Ludwig, C Dornmair, V T Moy, and H E Gaub 1995 Sensing specific molecular interactions with the atomic-force microscope *Biosens Bioelectron* 10 895–901

43 Proksch, R, T E Schaffer, J P Cleveland, R C Callahan, and M B Viani 2004 Finite optical spot size and position corrections in thermal spring constant calibration *Nanotechnology* 15 1344–1350

44 Tristram Nagle, S, Y Liu, J Legleiter, and J F Nagle 2002 Structure of gel phase DMPC determined by x ray diffraction *Biophys J* 83 3324–3335

45 Yang, J, and J Appleyard 2000 The main phase transition of mica supported phosphatidylcholine membranes *J Phys Chem B* 104 8097–8100

46 Nagle J F 1975 Chain model theory of lipid monolayer transitions *J Chem Phys* 63 1255–1261

47 Oncins G, S Garcia Manyes, and F Sanz 2005 Study of frictional properties of a phospholipid bilayer in a liquid environment with lateral force microscopy as a function of NaCl concentration *Langmuir* 21 7373–7379

48 Sturtevant, J M 1998 The effect of sodium chloride and calcium chloride on the main phase transition of dimyristoylphosphatidylcholine *Chem Phys Lipids* 95 163–168

49 Bockmann R A A Hac, T Heimburg, and H Grubmuller 2003 Effect of sodium chloride on a lipid bilayer *Biophys J* 85 1647–1655

50 Israelachvili J N 1991 Intermolecular and Surface Forces With Applications to Colloidal and Biological Systems Academic Press, London

51 Pera I, R Stark, M Kappl, H J Butt, and F Benfenati 2004 Using the atomic force microscope to study the interaction between two solid supported lipid bilayers and the influence of synapsin I *Biophys J* 87 2446–2455

52 Bockmann, R A, and H Grubmuller 2004 Multistep binding of divalent cations to phospholipid bilayers a molecular dynamics study *Angew Chem Int Ed Engl* 43 1021–1024

53 Pandit, S A, D Bostick, and M L Berkowitz 2003 Molecular dynamics simulation of a dipalmitoylphosphatidylcholine bilayer with NaCl *Biophys J* 84 3743–3750

54 Pandit, S A, and M L Berkowitz 2002 Molecular dynamics simulation of dipalmitoylphosphatidylserine bilayer with Na+ counterions *Biophys J* 82 1818–1827

55 Mukhopadhyay P, L Monticelli, and D P Tieleman 2004 Molecular dynamics simulation of a palmitoyl oleoyl phosphatidylserine bilayer with Na+ counterions and NaCl *Biophys J* 86 1601–1609

56 Sachs, J N, H Nanda, H I Petrache, and T B Woolf 2004 Changes in phosphatidylcholine headgroup tilt and water order induced by monovalent salts molecular dynamics simulations *Biophys J* 86 3772–3782

57 Kucerka, N, Y Liu, N Chu, H I Petrache S Tristram Nagle, and J F Nagle 2005 Structure of fully hydrated fluid phase DMPC and DLPC lipid bilayers using x ray scattering from oriented multilamellar arrays and from unilamellar vesicles *Biophys J* 88 2626–2637

58 Mason P C, J F Nagle, R M Epand, and J Katsaras 2001 Anomalous swelling in phospholipid bilayers is not coupled to the formation of a ripple phase *Phys Rev* 63 030902

59 Hawton, M H, and J W Doane 1987 Pretransitional phenomena in phospholipid/water multilayers *Biophys J* 52 401–404

60 Pasenkiewicz Gierula M, Y Takaoka H Miyagawa, K Kitamura, and A Kusumi 1997 Hydrogen bonding of water to phosphatidylcholine in the membrane as studied by a molecular dynamics simulation location geometry and lipid lipid bridging via hydrogen bonded water *J Phys Chem A* 101 3677–3691

61 Pasenkiewicz Gierula M Y Takaoka H Miyagawa, K Kitamura and A Kusumi 1999 Charge pairing of headgroups in phosphatidylcholine membranes a molecular dynamics simulation study *Biophys J* 76 1228–1240

62 Ho, C, and C D Stubbs 1997 Effect of n alkanols on lipid bilayer hydration *Biochemistry* 36 10630–10637

63 Rawicz, W, K C Olbrich T McIntosh, D Needham, and E Evans 2000 Effect of chain length and unsaturation on elasticity of lipid bilayers *Biophys J* 79 328–339

64 Olbrich, K W Rawicz D Needham and E Evans 2000 Water permeability and mechanical strength of polyunsaturated lipid bilayers *Biophys J* 79 321–327

65 Dimova, R I, C Dietrich, and B Pouligny 2000 Viscoelasticity of DMPC vesicle membranes near the main phase transition optical trapping manipulation of latex beads *Biophys J* 78 273A

66 Lee C H, W C Lin, and J Wang 2001 All optical measurements of the bending rigidity of lipid vesicle membranes across structural phase transitions *Phys Rev E* 64 020901

67 Heimburg, T 2000 A model for the lipid pretransition coupling of ripple formation with the chain melting transition *Biophys J* 78 1154–1165

68 Evans, E, and D Needham 1987 Physical properties of surfactant bilayer membranes thermal transitions, elasticity, rigidity, cohesion and colloidal interactions *J Phys Chem* 91 4219–4228

69 Needham D, and E Evans 1988 Structure and mechanical properties of giant lipid (DMPC) vesicle bilayers from 20°C below to 10°C above the liquid crystal crystalline phase transition at 24°C *Biochemistry* 27 8261–8269

70 Pabst, G, M Rappolt H Amenitsch, S Bernstorff, and P Laggner 2000 X-ray kinematography of temperature-jump relaxation probes the elastic properties of fluid bilayers *Langmuir* 16 8994–9001

5.4.6 Thermal response of Langmuir-Blodgett films of dipalmitoylphosphatidylcholine studied by Atomic Force Microscopy and Force Spectroscopy

G. Oncins[a], L. Picas[b], J. Hernandez-Borrell[b], S. Garcia-Manyes[a], F Sanz[a]

[a]Department of Physical Chemistry, Chemistry faculty, University of Barcelona and Institut de Bioenginyeria de Catalunya (IBEC), Martí i Franquès 1, 08028 Barcelona, Spain.

[b]Department of Physical Chemistry, Pharmacy Faculty, University of Barcelona, Joan XXIII Avenue, 08028 Barcelona, Spain.

Biophysical Journal (in press)

5.4.6.1 Summary

This work was conceived to respond a really specific question concerning the nature of the two consecutive phase transition processes observed in the paper presented in section 5.4.5. As pointed out by Leonenko et al.[359], it remained unclear if the double transition process corresponded to the individual melting of the leaflets that conform the bilayer or if it corresponded to two consecutive transition concerning the whole bilayer. Trying to answer this question, we prepared phospholipid LB monolayers and studied the transition process by means of variable temperature AFM and Force Spectroscopy. Our results can be summarized as follows.

- *Only one transition process is topographically observed in the interval of temperatures where two transitions are detected in bilayers. According to this, we concluded that each transition corresponded to the individual melting of the monolayers that compose the bilayer and not to a cooperative double transition*

which, possibly, would have given rise to two transition processes in the thermic study of the monolayer.

- *The trend of F_v vs. temperature curves is very similar to that obtained for bilayers but the measured F_v values are two orders of magnitude lower. This fact points out the incredible stability reached by bilayers respect to monolayers and why they have been chosen by nature to fulfill such demanding structural duties in cells.*

- *Experiments involving temperature cycles around T_M demonstrated that the transition from L_α to L_β is a nucleation and growth process, as hexagonal phospholipid microscopic structures were topographically detected by means of low interaction AM-AFM.*

Thermal response of Langmuir-Blodgett films of dipalmitoylphosphatidylcholine studied by Atomic Force Microscopy and Force Spectroscopy

Gerard Oncins[1], *Laura Picas*[2], *Jordi Hernández-Borrell*[2], Sergi *Garcia-Manyes*[1,3**], *Fausto Sanz*[1*]

[1]Department of Physical Chemistry, Chemistry faculty, University of Barcelona and Institut de Bioenginyeria de Catalunya (IBEC), Marti i Franques 1, 08028 Barcelona, Spain.

[2]Department of Physical Chemistry, Pharmacy Faculty, University of Barcelona, Joan XXIII Avenue, 08028 Barcelona, Spain.

*Corresponding author information: Tel.: 34-934021240; Fax: 34-934021231; E-mail: fsanz@ub.edu.

**Corresponding author information: Tel.: 01-2128549606; E-mail: sergi@biology.columbia.edu.

KEYWORDS

Membrane, phospholipid, force spectroscopy, AFM, phase transition.

[3]Present address: Department of Biological Sciences, Columbia University, 1212 Amsterdam Avenue, 10027 New York.

ABSTRACT

The topographic evolution of supported DPPC monolayers with temperature has been followed by AFM in liquid environment, revealing the presence of only one phase transition event around 46°C. This finding is a direct experimental proof that the two phase transitions observed in the corresponding bilayers correspond to the individual phase transition of the two leaflets composing the bilayer. The transition temperature and its dependency on the measuring medium (liquid saline solution or air) is discussed in terms of changes in van der Waals, hydration and hydrophobic/hydrophilic interactions, and it is directly compared with the transition temperatures observed in the related bilayers under the same experimental conditions. Force spectroscopy allows us to probe the nanomechanical properties of such monolayers as a function of temperature. These measurements show that the force needed to puncture the monolayers is highly dependent on the temperature and on the phospholipid phase, ranging from 120±4 pN at room temperature (liquid condensed phase) to 49±2 pN at 65°C (liquid expanded phase), which represents a two orders of magnitude decrease respect to the forces needed to puncture DPPC bilayers. The topographic study of the monolayers in air around the transition temperature revealed the presence of boundary domains in the monolayer surface forming 120° angles between them, thus suggesting that the cooling process from the liquid expanded to the liquid condensed phase follows a nucleation and growth mechanism.

INTRODUCTION

Physicochemical properties of biomembranes have been a matter of extensive research along the years. The elucidation of the transport processes across these structures as well as the understanding of the cell surface functionality has become common ground for interdisciplinary studies concerning physics, chemistry and biology. Although biomembranes are known to be heterogeneous in composition, phospholipid molecules are the predominant species. Therefore, the study of the physicochemical properties of phospholipid assemblies, both in the bilayer and monolayer forms, was shown to be crucial to the comprehension of model membranes.

Understanding the effect of mechanical stress on biological membranes is of fundamental importance since cells are known to naturally perform their function under the effect of a complex combination of forces (1). Indeed, the chemical composition of such membranes is the main responsible for determining their architecture, while guaranteeing the cell mechanical stability (2). In order to decipher the partial contribution of the membrane onto the overall cell mechanical integrity, several studies have been focused on the study of lipid bilayers, since they correctly mimic cell membranes up to an extent (3). So far, lipid bilayers have been extensively studied from a mechanical point of view. In the mesoscopic range, calorimetric experiments (4) and the development of techniques to manipulate giant vesicles have rendered experimental quantitative values for membrane curvature modulus and hydrodynamic shear viscosity (5-8). Down to the nanoscale, Atomic Force Microscopy (AFM) and related techniques have become really useful so as to characterize the topography of Supported Planar Bilayers (SPBs), that is, bilayers deposited on a flat surface, typically SiO_2, highly oriented pyrolitic graphite or mica (9-12) with nanometer resolution.

Besides, AFM in its Force Spectroscopy mode offers the possibility to extremely locally compress a supported bilayer with an AFM probe while precisely controlling the applied force with pN resolution. The analysis of the probe deflection during the compression process allows to study the elastic and plastic behavior of the bilayer. Several works have observed that the AFM probe can puncture the bilayer (13-15) provided that a certain threshold force is applied, giving rise to a discontinuity or 'jump' in the force-extension curve. The force at which the bilayer breaks (yield threshold force, F_y) can be considered as a fingerprint of the phospholipid phase, as it is intimately related with the intermolecular forces arisen between the phospholipid molecules, the substrate and the surrounding medium.

Along these lines, we recently reported (16) that an increase of the ionic strength in the measuring medium resulted in a higher F_y value due to a reduction of the area/lipid ratio as predicted by molecular dynamics calculations (17), thus highlighting the key role of electrostatic and van der Waals interactions in the bilayer compactness. Moreover, the interaction of the solvent with the phosphocholine polar heads and its key role in the overall bilayer stability has also been explored.

In a following work, the evolution of such F_y value has been related to the changes in the topographic evolution of DMPC and DPPC SPBs (18). Previous Differential Scanning Calorimetry (DSC) experiments on DPPC liposomes established that there is a main transition between two lamellar phases while raising the temperature, the solid-crystalline (L_β) and the liquid-crystalline (L_α) state, which are characterized by a quasi-hexagonal array packing (solid) and a higher molecular motion (liquid), respectively (19). The phase transition of DPPC SPBs on mica has also been topographically followed by means of variable temperature AFM (20), yielding two consecutive transitions. It was proposed that the first observed phase transition could correspond to the main L_β-L_α transition and that the second one could be adscribed to a further transition occurring at high temperatures yielding to a highly disordered fluid phase. By contrast, further studies suggested that the two transitions could correspond to the individual melting of the DPPC leaflets that compose the bilayer (21). The low temperature transition was related to the melting of the leaflet that is far from the surface (distal leaflet), less stable than the leaflet in contact with the mica surface (proximal leaflet). Force Spectroscopy experiments on DPPC SPBs have been directly related to the bilayer topographical changes as the temperature is changed (18). While in the L_β solid phase F_y decreases steadily as temperature increases reaching a minimum around transition temperature (T_M), in the L_α liquid phase F_y tends to plateau at a value slightly higher than that measured at T_M (18). These experiments concluded that F_y is an excellent experimental parameter to unambiguously characterize phospholipid phase transitions at the nanometer scale.

The nature of the two consecutive phase transitions observed in the bilayers could be elucidated by reproducing the same experiment with the respective monolayers. Furthermore, studying the thermal and mechanical response of single monolayers at the nanometer scale would help to shed light not only onto the phase transition phenomena, but also onto the more general study of the interactions arising between the involved interfaces (i.e., the surface, the monolayer and the liquid environment) and also between well-defined neighboring molecules. All these interactions are much more complex in the bilayer case, as curvature and asymmetry issues have to be taken into account.

DPPC monolayers have been extensively studied by using several methods such as light scattering (22-24) and spectroscopic techniques (25, 26). The use of fluorescent lipid analogs that dissolve preferentially in the liquid expanded (LE) phase permitted the morphological study of Langmuir monolayers while being compressed in the air-water interface (27). The shapes of the domains are characteristic for each pressure and therefore representative of the aggregation state of the DPPC monolayer. Similarly, by depositing the monolayer at the desired surface pressure onto a solid surface, AFM enables not only to visualize but to gain insight into the nanostructure of the DPPC monolayer (28-32). Interestingly, DPPC is one of the major constituents of the pulmonary surfactant, a coating with extremely demanding mechanical properties and where the air-water interface plays a biologically relevant role.

The aim of the present work is twofold. On the one hand, we aim to get further insight into the understanding of the physics underlying the two phase transitions described for SPBs. In brief, we are interested in elucidating whether the two consecutive phase transitions measured in variable temperature AFM experiments involve the separate melting of each of the two lipid leaflets composing the bilayer or if, on the contrary, two cooperative and consecutive phase transitions take place: the first one corresponding to the transition from the solid phase to liquid phase and the second one corresponding to the transition from liquid phase to liquid disordered phase. On the other hand, we aim to characterize the nanomechanical properties of Langmuir-Blodgett phospholipid monolayers using force spectroscopy. In particular, we aim to correlate the mechanical properties of such monolayers with their thermodynamics phase as a function of temperature. These experiments serve as the ideal platform to compare the mechanical properties of bilayers and monolayers under the same experimental conditions, and to test the additivity of the process. Last but not least, we endeavor to topographically characterize the reversible nucleation and growth processes during the first stages of phase formation, which is a direct signature of molecular reorganization involved during the main phase transition.

MATERIALS AND METHODS

Sample preparation

The lipid (Avanti Polar Lipids, AL, USA) was dissolved in chloroform-methanol (3:1, v/v) to a final concentration of 1 $mg \cdot mL^{-1}$. The preparation of the Langmuir-Blodgett (LB) films of DPPC was performed in a 312 DMC Langmuir-Blodgett trough manufactured by NIMA Technology Ltd. (Coventry, England). The trough was placed onto a vibration-isolated table (Newport, Irvine, CA, USA) and enclosed in an environmental chamber. The subphase (150mM NaCl + 20mM $MgCl_2$, pH~7.4 with 10mM Hepes/NaOH) was filtered with a Kitasato system (450 nm pore diameter) before use. The same buffer solution was used as liquid medium for imaging and force spectroscopy measurements. The resolution of surface pressure measurement was ±0.1 mN·m-1. In all experiments the temperature was maintained at 24.0±0.2°C by an external circulating water bath. Before each experiment, the trough was washed with chloroform and rinsed thoroughly with purified water. The cleanliness of the trough and subphase was ensured before each run by cycling the full range of the trough area and aspirating the air-water surface while at the minimal surface area, to zero surface pressure.

The corresponding aliquots of lipid were spread, drop by drop, onto subphase solution with a microsyringe Hamilton (Reno, NV). A period of 15 min was required to allow the solvent to evaporate before the experiment was started. The compression barrier speed to the final surface pressure was 5 $cm^2 min^{-1}$. LB films were transferred onto freshly cleaved mica, lifting the substrate at a constant rate of 1 $mm \cdot min^{-1}$. The transfer ratios were evaluated and were near the unity, indicating that the mica was practically covered with the monolayer.

Temperature-controlled AFM imaging

AFM experiments were performed with a Multimode microscope (Digital Instruments, Santa Barbara, CA) controlled by a Nanoscope IV electronics (Digital Instruments, Santa Barbara, CA). Due to the softness of the monolayers, images were acquired in tapping mode (TM-AFM). V-shaped Si_3N_4 cantilevers (OMCL TR400PSA, Olympus, Japan) with a nominal spring constant of 0.08 N/m were used in liquid operation, while beam-shaped silicon oxide tapping tips (37^{th} series B cantilever, MikroMasch, Portland, OR) with a nominal spring constant of 0.3 N/m were used in air. Images were acquired at minimum vertical force, that is, maximizing amplitude setpoint value while maintaining vibration amplitude as low as possible. Variable temperature experiments were performed attaching a temperature controller stage (Digital Instruments, Santa Barbara, CA) to the piezo-scanner. This device consists of a heating element placed below the magnetic sample holder and maintained at a fixed temperature (range: from room temperature up to 250°C, resolution: 0.1°C, accuracy: 3%, temperature drift: ±0.25°C). A water-ethanol fluid circuit refrigerates the piezo-scanner. It is very important to note that the heating element temperature is lower than the temperature of the sample surface; in order to operate in liquid environment, it is necessary to glue the mica surface to a Teflon disk that is glued to a metallic sample holder. The difference between the controller temperature and the real temperature of the sample surface can be as much as a 25% depending on the thickness of the Teflon and the epoxy glue. As a consequence, it is mandatory to calibrate sample holders individually before performing the measurements. To do that, a clean mica sheet is glued on the sample holder and a buffer droplet is spread on the surface as in a real experiment. Then, mica surface temperature is measured by a thermocouple (Cole Palmer thermocouple thermometer EW-91100-20 DigiSense; Resolution: 0.1°C, accuracy: ±0.25%, provided with Omega Precision Fine Wire Thermocouples) mounted in direct contact with the mica and a temperature ramp is performed so as to obtain the temperature factor between the controller temperature and the mica surface temperature. Upon imaging, temperature was varied from room temperature up to 80°C. Before acquiring every image, we waited 5 minutes in order to reach the equilibrium temperature of the system, although in ~1 min. temperature remained stable. After capturing an image, the tip was lifted 30 μm from the surface and the sample was heated to the next temperature.

Roughness measurements

Roughness can be expressed in several ways, being the mean roughness (R_a) and the root mean square (R_q) the most representative ones:

$$R_a = \frac{1}{N}\sum_{i=1}^{N} Z_i - Z_{ave} \quad (1)$$

where N is the total number of points within the given area, Z_i is the pixel height value in the z axis and Z_{ave} is the average of all Z_i values within the given area. R_q can be expressed as

$$R_q = \sqrt{\left(\frac{1}{N}\sum_{i=1}^{N} Z_i^2\right)} \quad (2)$$

The tendency of R_a and R_q as temperature increased is similar. Then, and for the sake of simplicity, only R_q measurements will be discussed but both values (R_a and R_q) are presented in Fig. 2.

Force spectroscopy

Force spectroscopy measurements in liquid media were performed using V-shaped Si_3N_4 tips (OMCL TR400PSA, Olympus, Japan) with a nominal spring constant of 0.08 N/m. However, individual spring constants were calibrated using the thermal noise routine (33) implemented in a MFP-1D atomic force microscope (Asylum Research, Santa Barbara, CA). Typically 150-200 force plots were recorded at each temperature and they were performed maintaining the laser spot in the same position on the cantilever in order to keep constant the corresponding photodetector sensitivity (V/nm), which was calculated for each temperature (34). All spectroscopy experiments were performed at a constant cantilever linear velocity of 0.5 μm/s in order to avoid any velocity-dependent effect. Tip radius was individually measured by imaging a faceted silicon grating (Mikromasch, Ultrasharp, TGG01, Silicon oxide 3 μm pitch), obtaining values ranging from 15 to 35 nm. Applied vertical forces (F) are given by $F = k_c \times \Delta$ where Δ is the cantilever deflection and k_c is the cantilever spring constant. The surface deformation is given as penetration (δ) evaluated as $\delta = z - \Delta$, where z represents the piezo-scanner displacement. X, Y, Z- piezo motion was calibrated with a DI silicon oxide grid (STR10-1800P), 180 nm deep, 10 μm pitch.

RESULTS AND DISCUSSION

LC-LE phase transition.

DPPC monolayers were transferred to a mica surface at a surface pressure of 30 mN/m, which is considered a biologically relevant surface pressure (35). To ensure the correct transfer onto the mica substrate, a freshly prepared sample was scratched with the AFM tip and a vertical distance of ca. 2 nm between the top of the layer and the bottom of the trench was obtained as it is shown in the supporting information. Although the height measurement was acquired in TM-AFM (contact mode was too aggressive for this monolayer), its thickness corresponds reasonably well with values elsewhere reported for DPPC (36, 37).

In order to investigate the topographic changes that DPPC monolayers undergo because of temperature changes, Fig. 1 shows a series of TM-AFM monolayer surface images in liquid environment as temperature is raised from 33.1°C up to 55.3°C, which corresponds to the temperature interval at which the phase transition of DPPC bilayers is expected. Fig. 1*a* and 1*b* were acquired at 33.1°C and 43.6°C respectively and the topographic images reveal a homogeneous and flat DPPC monolayer. As a reference, the T_M measured for DPPC liposomes in solution is 41.5°C (38). Upon raising the temperature up to 45.4°C, the topography undergoes a sudden roughness increase that can be already appreciated by visual inspection of Fig.1*c*. The same topographic features are still observed at 47.8°C (Fig. 1*d*). This topographic change is likely to correspond to the monolayer phase transition, which will be further investigated in a roughness analysis of the surface. With increasing temperature, the topography undergoes a new change as it can be observed in Fig. 1*e* and Fig. 1*f*, acquired at 51.6°C and 55.3°C respectively. In both images the sample appears to be totally flat again.

A monolayer phase transition implies a range of temperatures in which both LC and LE phases coexist. As LC and LE phases have different thickness values (39, 40), the images involving the coexistence of two phases should show a sharp increase in roughness with respect to the images in which the monolayer remains in a single phase (either LC or LE phase). The roughness analysis of the images shown in Fig. 1 is depicted in Fig. 2*a* in terms of R_q and R_a. At 33.1°C, R_q was 0.9 nm and this value decreased down to 0.6 nm at 43.6°C. This roughness decrease is consistent with an increase in phospholipid mobility. Indeed, fluorescence recovery after photobleaching experiments on egg-phosphocholine monolayers and bilayers (41) showed that phospholipid diffusion coefficient increases with temperature and that it also depends strongly both on the nature of the phospholipid polar head and the surface pressure of the monolayer (42, 43), mainly due to different electrostatic interactions between polar heads. Therefore, the decrease in roughness as temperature approaches T_M can be easily attributed to the promotion of the DPPC diffusion. Recent bending rigidity studies on DPPC giant liposomes showed that the value of this mechanical magnitude decreases steeply in the range of temperatures from the so-called pretransition temperature to T_M (5), according to the predictions of a previous model (44). These results were interpreted as the bilayer softening due to hydrocarbon chains melting, process that increases the homogeneity of the monolayer and, consequently, its surface smoothness (which would give rise to a decrease in roughness value).

As it is shown in figure 2*a*, between 43.6°C and 51.6°C, R_q increased by a factor of 3 (from ~0.7 nm up to ~2.5 nm). This observation may be accounted for as a result of the coexistence of the LC-LE phases, therefore implying a difference in the respective thickness value for the monolayer in both LC and LE phases. In-situ AFM variable temperature experiments performed by Feng et al. showed that the height decrease due to the transition of each of the leaflets present in a DPPC bilayer is 0.37 nm (45) and Charrier et al. (46) reported values of 0.4-0.7 nm for DMPC bilayers. This height change is attributed to the increase of the tilting angle of the DPPC molecule respect to the surface perpendicular as transition takes place (a 25° angle tilting was calculated for LC phase (47). The phase transition also implies the hydration of the polar heads as the molecules fluidize (40). Hence, the coexistence of two phases with different tilting angle (LC and LE phase) during the transition are very likely to be responsible for the increase in roughness observed between 43.6°C and 51.6°C in the case of the DPPC monolayers under study. At higher temperatures roughness decreases again, which is

consistent with the higher mobility of the LE phase respect to the LC phase. Therefore, roughness measurements seem to be a reliable experimental signature of the processes (phase transition) that the surface undergoes at the nanometric scale.

Four independent sets of experiments as those shown in Fig. 1 were performed, confirming that DPPC monolayers only undergo one phase transition in contrast with the two transitions observed for DPPC bilayers in previous works. The transition temperature range is reproducible from sample to sample, being always observed between 43 and 52°C. One phase transition in monolayers directly supports the hypothesis about the individual melting of the two DPPC leaflets being responsible for the two transitions observed in bilayers. The other suggested possibility, that is, two consecutive phase transitions involving each one the whole bilayer, would probably have also led to two transitions in the case of the monolayer.

Several transition temperatures were reported in the past for DPPC bilayers under different conditions. Values of 42.4°C and 44.8°C for SPBs adsorbed onto mica flakes were obtained by means of DSC (31), both transitions being above DPPC liposomes T_M(41.5°C), and were attributed to the individual melting of the two DPPC leaflets. The higher transition temperatures of SPBs with respect to the non-supported liposomes were interpreted as a stabilizing effect due to the electrostatic interactions arisen between the bilayer and the mica surface. Other authors obtained in situ AFM evidence of two DPPC SPBs phase transitions in water. Leonenko et al. (20) reported a temperature range of 42°C-60°C, while Keller et al. (21) reported values from 37.8°C to 53.5°C for a mixture of DPPC and another phosphocholine. We have recently observed two transitions between 44.8°C-59.4°C in experiments that mimic a physiological environment (18), which is also used here. Then, and assuming that the two transitions correspond to the individual melting of the two DPPC leaflets, the high temperature transition in the bilayer should correspond to the LC-LE transition of the proximal leaflet. Fig. 2*b* shows for comparison the roughness analysis of a series of DPPC bilayer topographic images performed at variable temperature (18). Comparing the phase transition temperature intervals, marked with gray rectangles in fig. 2*a* and 2*b*, it can be seen that the DPPC monolayer transition lies between the two transitions observed in the DPPC bilayer. Comparing the proximal leaflet transition with the monolayer transition is interesting because both the proximal leaflet and the monolayer share the same phosphocholine-mica interface but have a different medium sorrounding the alkyl chain (proximal leaflet is covered by another phospholipid leaflet with alkyl chains facing downwards while the monolayer is surrounded by an aqueous solution). As shown in Fig. 1, monolayer transition occurs from 43.6 to 51.6°C, while proximal leaflet transition takes place between 52°C and 59°C (18). This fact, besides the experimental evidence of a strong coupling between the two DPPC leaflets during phase transition (19) and the roughness measurements that place the monolayer transition temperature between the two transitions observed in the bilayer, suggests that the distal monolayer stabilizes the proximal monolayer because of van der Waals interactions between the alkyl chains of the two monolayers, providing a stable, highly hydrophobic environment. Moreover, the monolayer has an unstable hydrophobic-hydrophilic interface because of the contact between the alkyl chains and the aqueous environment (48). In order to experimentally test the importance of the alkyl chains-medium interface in the transition temperature, several DPPC monolayers were imaged at variable temperature, but now in air. As in liquid, one transition was observed but now T_M ranged from 48°C to 51°C (3 different experiments with freshly prepared samples). This implies a reduction of the transition temperature range (from 43°C-51°C in liquid to 48°C-51°C in air)

and also a ~4°C increase in the mean transition temperature. Air, which is more hydrophobic than an aqueous solution, stabilizes the alkyl chains of the DPPC monolayer, which translates into a T_M increase. These results experimentally prove the key role that interactions arisen in the sample interphase play in the physicochemical properties of molecularly thin structures, as is the case of DPPC monolayers.

Topography of DPPC domain edges at variable temperature imaged in air

In order to explore the homogeneity of the extracted Langmuir-Blodgett films and to study the topographic changes around TM, the same experiment presented in Fig. 1 was repeated although this time in air conditions. Fig. 3a shows a DPPC monolayer at room temperature after LB film extraction and deposition imaged by TM-AFM. This image is similar to the one obtained in aqueous buffer environment (Fig. 1a), although now the presence of geometrical patterns on the monolayer is evident (some of them were marked with black arrows in Fig.3a to guide the eye). As temperature was increased beyond TM (Fig. 3b), these features disappeared, yielding a flat surface. Then, the temperature was decreased to 30°C (Fig. 3c) and new geometrical patterns appeared again. The presence of patterns in the LC phase and its disappearance in the LE phase suggests that they form part of the structure of the monolayer and that they are related to the LC-LE phase transition process. Interestingly, as the cartoon in Fig. 3d shows, the patterns observed in Fig. 3c form 120° angles between them. Several works have been devoted in the past to the study of domain boundaries in organic monolayers (49), phospholipid structures (44, 50) and, specifically, DPPC LBs morphology has been studied during compression experiments. McConlogue (51) showed AFM images of DPPC structures on liquid subphase extracted at surface pressures ranging from 3.8 mN/m to 7.5 mN/m and corresponding to the region of LE-LC phase coexistence. As pressure increased, the LC phase domains grew at expense of the LE phase. Finally, only a film of LE phase separated the LC nuclei, which formed angles ca. 120° between them. As noted, the repulsive interaction between the growing LC phase nuclei can be counteracted if enough pressure is applied (56), which leads to the final fusion of these solid nuclei. Our results suggest that if a high enough pressure is applied (30 mN/m in our case), LC domains can merge and the domain boundaries between different nuclei are the patterns observed in Fig. 3a and Fig. 3c. Indeed, hexagonal shapes were recently reported (45) during the melting of DPPC bilayers monitored by in-situ AFM observations and attributed to the phospholipid intrinsic molecular packing.

To the best of our knowledge, this is the first time that domain boundaries have been imaged in a phospholipid monolayer. The structure of the domain boundary is still unclear, but it is likely to assume that it is formed by disordered DPPC molecules that were forced to occupy the mismatch between colliding LC phase domains, as it was suggested after electron diffraction measurements on phospholipid bilayers (57). In our experiments, as the temperature increases above T_M and the monolayer changes from LC to LE phase, DPPC molecules mobility increases and the domain boundaries disappear (Fig. 3*b*). Interestingly, the presence of domain boundaries was not observed in DPPC monolayers imaged in liquid environment at any temperature, which suggests that the aqueous medium relaxes the mechanical tension formed in the domain boundaries as the monolayer is compressed from LE to LC phase (mechanical extraction process) or the phase transition from LE to LC phase takes place (temperature controlled process). As noted before, the presence of water destabilizes the alkyl chain-medium interphase, thus reducing the phase transition temperature respect an air interphase. Therefore, it is

reasonable to think that LC phase mobility is higher in aqueous medium, leading to defect-free LC domain boundaries. An important conclusion from our findings is that the temperature controlled solidification process undergone in temperature controlled AFM experiments leads to the presence of domain boundaries, as well as the surface pressure controlled solidification process (compression in the LB trough), that is, in both cases, a nucleation and growth of the LC phase process takes place. Future work should be done to establish the dependence of shape and size as a function of LB compression rate and cooling rate, as well as to explore the presence of domain boundaries in different polarity liquid media in order to discern the nature of the interphase forces responsible for the monolayer relaxation.

Force spectroscopy at variable temperature

So far, the topographic changes that the monolayer undergoes as a function of temperature have been studied. Roughness analysis of the topographic images reveals to be a sensitive tool able to detect the main transition temperature undergone by the monolayer. However, roughness analysis provides only information about the topographic changes that take place in the surface. Rather, force spectroscopy through force-extension curves allows to gather additional quantitative information regarding the interaction forces arisen between neighboring molecules and also to gain further insight into the mechanical properties of the substrate with pN and subnanometric resolution. The force at which the substrate breaks, the so-called threshold force, F_y, is the maximum force that the substrate is able to withstand before breaking, i.e., it marks the end of the elastic regime and the onset of the plastic deformation. In the case of lipid bilayers, we have shown that F_y is able to accurately fingerprint the bilayer phase transitions, since they involve a drastic molecular rearrangement, thus implying a change in the intermolecular interaction forces. In order to further understand the phase transition process in the case of the studied DPPC monolayers, we have performed multiple vertical force vs. piezo displacement (*FvD*) curves on the monolayers, yielding experimental curves as the one shown in Fig. 4. In this force plot, the force applied on the sample is recorded against the tip-sample distance (*FvP* curve). This curve is obtained from the raw force vs. piezoelectric displacement curve shown in the inset as described in the Materials and Methods section. In each curve, the vertical force, which is proportional to the cantilever deflection, remains 0 prior to the contact between tip and sample, marked as point *1*. Then, vertical force increases as the tip compresses the monolayer until F_y value is reached and the tip penetrates the monolayer (point *2*). The jump in the force-penetration curve can be directly correlated with the thickness of the monolayer (55, 58). The initial region of the *FvP* curve in Fig. 4 corresponds to the physical compression of the monolayer and to the electrostatic interaction arisen because of the slightly negative charge of the tip (56) and the weak electrical double layer promoted by the phosphocholine zwitterionic headgroups and the mica surface. Derjaguin-Landau-Verwey-Overbeek theory (DLVO) was applied elsewhere (16) to estimate the forces arising between a 1,2-dimyristoyl-sn-glycero-3-phosphocholine (DMPC) bilayer and a Si_3N_4 tip as a function of the ionic strength of the medium. Due to the low charge of the Si_3N_4 tip (0.032 C/m^2) (56), the interaction forces are in the pN range in bilayers. In the case of DPPC monolayers, interaction forces are much lower because phosphocholine polar headgroups, which are responsible for the formation of a charged interface between the membrane and the solution in bilayers, are directed towards mica in monolayers while the apolar alkyl tails, showing no dipolar moment and consequently not structuring an electric double layer, are exposed to the aqueous medium. As a result, the effect of electrostatic interactions is negligible in DPPC monolayers. Nevertheless, as the electrical double

layer is practically independent of temperature for small temperature increments, F_y variation with temperature is only due to monolayer structural changes, that is, to its mechanical properties. Finally, the breakthrough event is detected as a sudden 2-3 nm penetration, which compares well with the nominal thickness of the DPPC monolayer (57) and to our scratching measurements. After penetration, the tip contacts the mica that is beneath the monolayer (13, 58) and the slope of the exerted *FvP* curve tends to ∞.

Fig. 5*a* shows the dependence of F_y vs. temperature. *FvD* curves were performed from room temperature to 65°C at ~8°C intervals. Each point is the F_y average value of 150-200 individual measurements performed in several different spots on the sample surface and the error bars stand for $2\sigma/\sqrt{N}$, being σ the standard deviation and N the number of measurements (examples of the F_y histograms obtained are depicted in Fig. 5*b*, corresponding to measurements performed at 5*b.1*) 21.2°C, 5*b.2*) 46.4°C and 5*b.3*) 67.7°C. This experiment was performed several times on different freshly prepared samples obtaining similar results. In order to relate F_y variations with the phase transitions detected in topographic images shown in Fig. 1, Fig. 5*a* has been divided into three regions as in a previous work (18): LC phase, phase transition range and LE phase. At room temperature, F_y is 120±4 pN. This force steadily decreases as temperature increases, reaching 88±3 pN at 38°C near the upper temperature limit of the LC phase. During the phase transition there is a further diminution of F_y value, reaching 53±2 pN at 53°C. Finally, after completing the transition, the monolayer stays in a LE phase and F_y stabilizes around 49±2 pN at 65°C.

Three important conclusions arise from these data; Firstly, F_y value is much higher in the LC phase than in the LE phase. Secondly, F_y continuously decreases as temperature increases, both in the LC phase and during the transition and thirdly, F_y ranges roughly from ~120 to ~40 pN for DPPC monolayers, while it ranges from ~25 nN to ~7 nN in DPPC bilayers in the same range of temperatures and under the same experimental conditions.

The two first conclusions are in agreement with a previous work concerning DPPC bilayers (16), where a similar trend was observed and attributed to the weakening of lateral interactions between alkane chains due to thermal energy and to the reduction of water bridges (59, 60) and electrostatic interactions between polar heads during the phase transition. The weakening of lateral alkyl-alkyl interactions results in an increase in the area per molecule, that is, a decrease in the compactness of the monolayer, which translates into an increase in the molecular mobility as previously commented in Fig. 2 (61), where LC phase roughness decreases before reaching the phase transition.

Consequently, the weakening of lateral interactions between molecules translates into a F_y reduction. Different factors account for the notorious difference in mechanical properties between DPPC monolayers and bilayers; first of all, the monolayers expose the hydrophobic alkyl chains towards the aqueous solution. It has been experimentally demonstrated that the interactions water-alkyl chains are 10 times weaker than the interaction between water molecules (48), leading to an interphase that destabilizes the monolayer. Conversely, the bilayer exposes the polar zwitterionic headgroups towards the solution, which is a favorable interaction in terms of hydrophilicity. Besides, ions also play an important role stabilizing phosphocholine heads (16), as it has been also studied by molecular dynamics, concluding that up to 3 phosphate moieties can be coordinated by each Na^+ ion (17). Additional experimental observations

concluded that the self-diffusion of 1-palmitoyl-2-oleoylphosphatidylcholine decreases due to the presence of NaCl in the medium (62) and that polar headgroups orientation is also perturbed (63), which confirms the key role that free charges play in the stability of bilayers. Another factor that improves bilayer cohesion is the hydrophobic interaction between the alkyl chains of the two leaflets, as detected studying lipid diffusivity by means of fluorescence techniques (64). Nevertheless, this can be a minor issue in the stability of the bilayer, as lipid diffusion studies concerning DPPC bilayers (52) suggest that the hydrophobic interactions between the two lipid leaflets are weaker than the interactions between the lower leaflet and the (silica) substrate.

In order to relate the DPPC monolayer structure with the measured F_y values, different interactions should be considered, namely electrostatic and van der Waals forces. Because of the mica surface negative charge (53) and the positive charge of the choline headgroups (phosphocholine is a zwitterionic headgroup with the choline positive charge facing towards the mica surface), electrostatic interactions arise. Nevertheless, it was observed by several techniques such as neutron reflectivity (65, 66) and fluorescence interference-contrast microscopy (67, 68) that there is a sandwiched water layer with a thickness ranging from 10 to 30 Å between the substrate and the phospholipid bilayers. Related experiments concerning the effect of pH and ionic strength in bilayer spreading on oxides revealed that the equilibrium distance between the polar heads and the substrate surface is ~1 nm (69) and that this gap is full of water molecules. Although there is some controversy about the level of water organization forced by the substrate (70), the presence of structured water on the surface of mica and silica was proved by scanning polarization force microscopy, sum-frequency-generation vibrational spectroscopy (71) and Monte Carlo simulations (72). As a consequence, the water layer between the substrate and the DPPC polar headgroups provides fluidity and mobility to the bilayer (3, 45, 69). As a first approximation and due to the screening effect of the water sandwiched underneath the monolayer, electrostatic interactions between mica and DPPC polar heads have been neglected in this study.

The electrostatic interactions arisen between polar headgroups have been discussed in several simulation works, suggesting that ions can penetrate the polar headgroups in order to screen the charges of the choline and phosphate moieties (17,62,63, 73). Nevertheless, as the calculation of these electrostatic interactions is out of the scope of this work and for the sake of simplicity, van der Waals forces between hydrocarbon chains will be considered as the most representative interaction between DPPC molecules.

Van der Waals interaction between hydrocarbon chains (E_{VdW}) can be expressed as (71):

$$E_{1,dW} = \frac{3\alpha_0^2 h\nu}{4(4\pi\varepsilon_0)^2}\left[\frac{6}{\sigma^2} + \frac{12}{\left[\sigma^2 + l^2\right]^3} + \frac{12}{\left[\sigma^2 + (2l)^2\right]^3} + \ldots\right]\frac{N_0}{2} \qquad (3)$$

being α_o the polarizability, ε_o the vacuum permittivity, σ the distance between 2 equivalent $-CH_2$ groups in adjacent molecules, l the distance between consecutive $-CH_2$ groups in the same hydrocarbon chain and N_o Avogadro's number. As the monolayer was extracted at 30 mN/m, the area/DPPC molecule is 54.7 $Å^2$ in a hexagonal lattice (36, 45, 75, 76). As each DPPC molecule

has two hydrocarbon chains, it has been considered that each chain occupies an area equal to 54.7/2 $Å^2$. Circles in Fig. 6*a* correspond to the molecular DPPC area in the monolayer and the black dots represent the hydrocarbon chains seen from above, while Fig. 6*b* shows a side view of the same structure. The alignment of the chains in the Y direction respond to the packing optimization of van der Waals interactions, which has been mostly studied in alkanethiols (80-82) and alkanesilanes (83). Van der Waals forces considered in this study include the interactions between a $-CH_2$ group and the 6 adjacent $-CH_2$ groups in the same plane and also the interaction with the $-CH_2$ groups that are 1 and 2 planes higher and lower. This interaction was multiplied by a factor of 2 because there are two chains in each molecule. The interactions between $-CH_2$ groups in the same molecule were not considered because only intermolecular energies are to be estimated. The resulting energy was multiplied by 16, which is the length of the DPPC hydrocarbon chains, obtaining E_{VdW} = 19.4 KJ/mol.

The experimental energy needed to puncture the monolayer during force spectroscopy measurements (*E*) can be calculated as

$$E = F_y * \delta \tag{4}$$

At room temperature, DPPC monolayer F_y is 120±4 pN and δ is 2.4 nm (36, 37), so E is 0.29 10^{-18} J. Although this energy is mainly consumed in the monolayer breakthrough process, part of it is possibly dissipated through non-conservative processes such as viscous damping or hysteresis effects (81). Energy dissipation was measured in dynamic force microscopy experiments concerning different kinds of surfaces and tip configurations, yielding values in the eV range (82). As a consequence, it is reasonable to think that in force spectroscopy experiments similar processes will take place. Nevertheless, and due to the semi-quantitative nature of the energetic calculations proposed in this work, energy dissipation has not been accounted for.

To estimate the contact area between tip and monolayer and the number of molecules affected by the tip during spectroscopy experiments, Hertz contact model has been applied. In a previous work (16), we demonstrated that a contact mechanics model based on the coupling of n springs is more realistic than Hertz model when it comes to explain the elastic region of a phospholipid bilayer prior to indentation (83). Nevertheless, and to calculate the contact area between tip and sample at low loads, Hertz model is accurate enough because it does not consider long range forces arisen between tip and sample, which is the case of our experiments, as no jump to contact was detected in *FvD* curves (Fig. 4) The hertzian contact area (A) is expressed as

$$A = \pi(RF/K)^{2/3} \tag{5}$$

where R is the tip radius, F is the vertical force and K is the combined elastic moduli

$$K = 4/3\ ((1-\nu_1^2)/E_1 + (1-\nu_2^2)/E_2)^{-1} \tag{6}$$

where ν_1 and ν_2 are the Poisson ratios of the tip and the sample, 0.2 (84) and 0.5 respectively (14, 85), and E_1 and E_2 are the Young's moduli of the tip and the sample, 280 GPa (84) and 15 MPa (86). Considering the experimental area/DPPC molecule and F_y = 120 pN, the number of

affected molecules is ~205 for R = 15nm and ~360 for R = 35 nm. These R values are the maximum and minimum tip radius measured in the presented experiments and can be considered as typical upper and lower limits for the vast majority of force spectroscopy studies. Dividing the total applied energy during the breakthrough process by the number of affected molecules, a breakthrough energy (E_b) of 0.8 KJ/mol for R_{15nm} and 0.5KJ/mol for R_{35nm} is obtained. It was previously shown that the E_{VdW} is 19.4 KJ/mol, an order of magnitude bigger than E_b. This fact seems to suggest that the energy necessary to break the DPPC monolayer is 20-40 times lower than the van der Waals interaction between all the hydrocarbon chains of the molecules in the penetration affected area. Regarding these results, it is reasonable to think that, in order to puncture the monolayer, it is not necessary to break all the interactions between all the molecules but only a fraction of them, so E_b should be lower than E_{VdW}. As an attempt to explain how the monolayer reacts to the pressure, Fig. 7 shows two possible monolayer rupture mechanisms. Fig. 7*a* represents an upper view of the hexagonal DPPC lattice and a circle that encloses the hertzian area of contact between the tip and the sample. The simplest rupture model proposed is a straight line (dotted line in Fig. 7*a* and 7*b*). Possibly, the presence of a vacancy or any defect in the structure would be the starting point of the monolayer rupture process. The fragile nature of phospholipid structures has been suggested before (16, 87), mainly because of the kind of breakthrough seen in force spectroscopy experiments, which always implies a sudden penetration, more similar to a fragile brittle fracture than to the compression of a soft material. The breakthrough event in the *FvP* curve shown in Fig. 4 occurs at a certain F_y and it is a sudden all-or-none process, as the tip penetrates the monolayer in a one-step mechanism. Another possibility would be a monolayer failure along the contact area perimeter (circle in fig. 7*a* and 7*b*). Both the linear and perimeter rupture imply the disruption of a certain number of van der Waals interactions, which depends on the contact area. Concerning the number of alkyl chain interactions broken during penetration, these models can be considered as extreme possibilities, so the real process is possibly a combination of both. Table 1 summarizes the percentage of van der Waals interactions broken in the linear ($\%R_l$) and circular model ($\%R_p$) with respect to the total number of van der Waals interactions present in the whole contact area. Depending on the rupture model and R, $\%R_l$ and $\%R_p$ range from 5-16%, so this percentage is an estimation of the van der Waals interactions broken during the penetration process respect to the total number of van der Waals interactions. Table 1 also shows the relationship between E_b and E_{VdW}, which is the ratio between the energy used to break the monolayer and the total van der Waals interactions between the hydrocarbon chains ($\%(E_b/E_{VdW})$). This ratio ranges from 3-4%. The similarity between the ratios $\%R_l$, $\%R_p$ and $\%(E_b/E_{VdW})$ suggests that the linear and circular models are consistent with experimental data. As a consequence, it can be considered that, although several forces are involved in the cohesion of DPPC monolayers, inter-chain van der Waals interactions play a key role in the mechanical properties of DPPC monolayers and that electrostatic interactions between polar heads and between choline groups and mica surface can be neglected as a first approximation. Of course, the nature of the calculations presented in this work can not discriminate between the two proposed models but it provides a framework to study the behavior of phospholipid monolayers under compression. Further studies exploring the effect of different polar heads and different alkyl chains length will provide a deeper insight in the effect that electrostatic and van der Waals forces play in the cohesion and mechanical response of phospholipid monolayers and bilayers.

CONCLUSIONS

Langmuir-Blodgett DPPC monolayers extracted at 30mN/m were imaged *in situ* by variable temperature TM-AFM. The experiments performed in buffer environment revealed that only one phase transition takes place around T_M, which suggests that the two transitions observed in DPPC bilayers in the same buffer media correspond to the melting of the two separate phospholipid leaflets. DPPC monolayer T_M lies between the two transitions observed in DPPC bilayers. We propose that the monolayer can be compared to the leaflet in contact with the substrate in the bilayer structure (high temperature transition) but destabilized by the water-alkyl chains interphase and the lack of the stabilizing hydrophobic interaction between the alkyl chains of the two phospholipid leaflets that form the bilayer. DPPC monolayer T_M increases in air, where a favorable air-alkyl chains interphase arises, which further supports this conclusion. The topographic study of DPPC monolayers imaged in air revealed the presence of 120° LC phase domain boundaries both created during the mechanical compression in the LB trough and during the cooling from LE to LC phase. The boundaries disappear above T_M and are recovered if the sample is cooled again to room temperature, suggesting that a nucleation and growth mechanism is responsible for the formation of the LC phase when cooling from the LE phase.

The mechanical study by force spectroscopy showed F_y in the pN range for DPPC monolayers, two orders of magnitude lower than those obtained in DPPC bilayers. Nevertheless, the overall trend of monolayers and bilayers is similar upon raising temperature: In the solid phase, F_y decreases as temperature increases, while it stablizes at a lower value in the liquid phase. In order to relate F_y values with DPPC monolayers structure, a simple geometric model concerning van der Waals interactions between the phospholipid alkane chains has been proposed. Applying Hertz contact mechanics, the energy/DPPC molecule applied on the monolayer during penetration experiments was calculated and assuming simple models for the monolayer rupture (namely across a straight line or around the perimeter of the contact area between tip and sample), a good accordance between the experimental data and the geometric model was found.

This work paves the way for more complex studies involving mixed monolayers systems, where temperature-controlled AFM imaging could shed light on the different transition processes that monolayers (and bilayers) undergo when mixing miscible or immiscible phospholipid molecules. Besides, force spectroscopy proves to be a suitable technique to identify different phospholipid phases, as F_y value is highly dependent on the phospholipid structure, and can be used to explore the different intermolecular interactions arisen in biological membranes.

ACKNOWLEDGMENTS

G.O. and L.P. are recipients of a 'Recerca i Docència' fellowship from the University of Barcelona. This work was supported by grant CTQ2004-08046 from Ministerio de Ciencia y Tecnología (MCYT) and SGR00664 (Generalitat de Catalunya) of Spain.

FERENCES

1. Vogel, V. and M. Sheetz 1983. Local force and geometry sensing regulate cell functions. Nature Rev. 7(4), 265-275.

2. Sheetz, M. P., J.E. Sable and H.G. Dobereiner 2006. Continuous membrane-cytoskeleton adhesion requires continuous accommodation to lipid and cytoskeleton dynamics. Annu. Rev. Biophys. Biomol. Struct. 35, 417-434.

3. Sackmann, E. 1996. Supported membranes: Scientific and practical applications. Science. 271, 43-48.

4. Heimburg, T. 1998. Mechanical aspects of membrane thermodynamics. estimation of the mechanical properties of lipid membranes close to the chain melting transition from calorimetry. Biochim. Biophys. Acta. 1415, 147-162.

5. Lee, C. H., W.C. Lin and J. Wang 2001. All-optical measurements of the bending rigidity of lipid-vesicle membranes across structural phase transitions. Phys. Rev. E. Stat. Nonlin Soft Matter Phys. 64, 020901.

6. Dimova, R., B. Pouligny and C. Dietrich 2000. Pretransitional effects in dimyristoylphosphatidylcholine vesicle membranes: Optical dynamometry study. Biophys. J. 79, 340-356.

7. Evans, E. and D. Needham 1987. Physical-properties of surfactant bilayer-membranes - thermal transitions, elasticity, rigidity, cohesion, and colloidal interactions. J. Phys. Chem. 91, 4219-4228.

8. Meleard, P., C. Gerbeaud, P. Bardusco, N. Jeandaine, M.D. Mitov and L. Fernandez-Puente 1998. Mechanical properties of model membranes studied from shape transformations of giant vesicles. Biochimie. 80, 401-413.

9. Mueller, H., H.J. Butt and E. Bamberg 1999. Force measurements on myelin basic protein adsorbed to mica and lipid bilayer surfaces done with the atomic force microscope. Biophys. J. 76, 1072-1079.

10. Zasadzinski, J. A., C.A. Helm, M.L. Longo, A.L. Weisenhorn, S.A. Gould and P.K. Hansma 1991. Atomic force microscopy of hydrated phosphatidylethanolamine bilayers. Biophys. J. 59, 755-760.

11. Egger, M., F. Ohnesorge, A.L. Weisenhorn, S.P. Heyn, B. Drake, C.B. Prater, S.A.C. Gould, P.K. Hansma and H.E. Gaub 1990. Wet lipid protein membranes imaged at submolecular resolution by atomic force microscopy. J. Struct. Biol. 103, 89-94.

12. Garcia-Manyes, S., G. Oncins and F. Sanz 2006. Effect of pH and ionic strength on phospholipid nanomechanics and on deposition process onto hydrophilic surfaces measured by AFM. Electrochim. Acta. 51, 5029-5036.

13. Franz, V., S. Loi, H. Muller, E. Bamberg and H.H. Butt 2002. Tip penetration through lipid bilayers in atomic force microscopy. Colloids Surf. B. 23, 191-200.

14. Kunneke, S., D. Kruger and A. Janshoff 2004. Scrutiny of the failure of lipid membranes as a function of headgroups, chain length, and lamellarity measured by scanning force microscopy. Biophys. J. 86, 1545-1553.

15. Liang, X. M., G.Z. Mao and K.Y.S. Ng 2004. Probing small unilamellar EggPC vesicles on mica surface by atomic force microscopy. Colloids Surf. B. 34, 41-51.

16. Garcia-Manyes, S., G. Oncins and F. Sanz 2005. Effect of ion-binding and chemical phospholipid structure on the nanomechanics of lipid bilayers studied by force spectroscopy. Biophys. J. 89, 1812-1826.

17. Bockmann, R. A., A. Hac, T. Heimburg and H. Grubmuller 2003. Effect of sodium chloride on a lipid bilayer. Biophys. J. 85, 1647-1655.

18. Garcia-Manyes, S., G. Oncins and F. Sanz 2005. Effect of temperature on the nanomechanics of lipid bilayers studied by force spectroscopy. Biophys. J. 89, 4261-4274.

19. Yang, J. and J. Appleyard 2000. The main phase transition of mica-supported phosphatidylcholine membranes. J Phys Chem B. 104, 8097-8100.

20. Leonenko, Z. V., E. Finot, H. Ma, T.E. Dahms and D.T. Cramb 2004. Investigation of temperature-induced phase transitions in DOPC and DPPC phospholipid bilayers using temperature-controlled scanning force microscopy. Biophys. J. 86, 3783-3793.

21. Keller, D., N.B. Larsen, I.M. Moller and O.G. Mouritsen 2005. Decoupled phase transitions and grain-boundary melting in supported phospholipid bilayers. Phys. Rev. Lett. 94, 025701.

22. Bonnerot, A., P.A. Chollet, H. Frisby and M. Hoclet 1985. Infrared and electron-diffraction studies of transient stages in very thin langmuir-blodgett films. Chem. Phys. 97, 365-377.

23. Bohm, C., R. Steitz and H. Riegler 1989. Temperature-dependent electron-diffraction studies of cadmium arachidate monolayers and multilayers. Thin Solid Films. 178, 511-517.

24. Peterson, I. R., R. Steitz, H. Krug and I. Voigtmartin 1990. An investigation of the spot profiles in transmission electron-diffraction from langmuir-blodgett-films of aliphatic chain compounds. Journal De Physique. 51, 1003-1026.

25. Rabe, J. P., J.D. Swalen and J.F. Rabolt 1987. Order-disorder transitions in langmuir-blodgett-films .3. polarized raman studies of cadmium arachidate using integrated optical techniques. J. Chem. Phys. 86, 1601-1607.

26. Nakanaga, T., M. Matsumoto, Y. Kawabata, H. Takeo and C. Matsumura 1989. Observation of ftir-pa spectra of langmuir-blodgett films of cadmium arachidate on glass plates. Chem. Phys. Lett. 160, 129-133.

27. Nag, K., C. Boland, N. Rich and K.M. Keough 1991. Epifluorescence microscopic observation of monolayers of dipalmitoylphosphatidylcholine: Dependence of domain size on compression rates. Biochim. Biophys. Acta. 1068, 157-160.

28. Schwartz, D. K., J. Garnaes, R. Viswanathan and J.A.N. Zasadzinski 1992. Surface order and stability of langmuir-blodgett-films. Science. 257, 508-511.

29. Schwartz, D. K., R. Viswanathan, J. Garnaes and J.A. Zasadzinski 1993. Influence of cations, alkane chain-length, and substrate on molecular order of langmuir-blodgett-films. J. Am. Chem. Soc. 115, 7374-7380.

30. Viswanathan, R., L.L. Madsen, J.A. Zasadzinski and D.K. Schwartz 1995. Liquid to hexatic to crystalline order in langmuir-blodgett films. Science. 269, 51-54.

31. Bourdieu, L., O. Ronsin and D. Chatenay 1993. Molecular positional order in langmuir-blodgett-films by atomic force microscopy. Science. 259, 798-801.

32. Zhai, X. and J.M. Kleijn 1997. Molecular structure of dipalmitoylphosphatidylcholine langmuir-blodgett monolayers studied by atomic force microscopy. Thin Solid Films. 304, 327-332.

33. Florin, E. L., M. Rief, H. Lehmann, M. Ludwig, C. Dornmair, V.T. Moy and H.E. Gaub 1995. Sensing specific molecular-interactions with the atomic-force microscope. Biosens. Bioelectron. 10, 895-901.

34. Proksch, R., T.E. Schaffer, J.P. Cleveland, R.C. Callahan and M.B. Viani 2004. Finite optical spot size and position corrections in thermal spring constant calibration. Nanotechnology. 15, 1344-1350.

35. Cevc, G.andD. Marsh 1987. Phospholipid Bilayers. Physical Principles and Models. Wiley-Interscience, New York.

36. Chunbo, Y., D. Desheng, L. Zuhong and L. Juzheng 1999. Molecular positional order in a dipalmitoylphosphatidic acidLangmuir–Blodgett monolayer by atomic force microscopy. Colloids Surf. A. 150, 1-6.

37. Greenhall, M. H., P.J. Lukes, M.C. Petty, J. Yarwood and Y. Lvov 1994. The formation and characterization of langmuir-blodgett-films of dipalmitoylphosphatidic acid. Thin Solid Films. 243, 596-601.

38. Huang, C. H. and S.S. Li 1999. Calorimetric and molecular mechanics studies of the thermotropic phase behavior of membrane phospholipids. Biochim. Biophys. Acta. 1422, 273-307.

39. Watry, M. R., T.L. Tarbuck and G.I. Richmond 2003. Vibrational sum-frequency studies of a series of phospholipid monolayers and the associated water structure at the vapor. J Phys Chem B. 107, 512-518.

40. Jyoti, A., R.M. Prokop, J. Li, D. Vollhardt, D.Y. Kwok, R. Miller, H. Mohwald and A.W. Neumann 1996. An investigation of the compression rate dependence on the surface pressure-surface area isotherm for a dipalmitoyl phosphatidylcholine monolayer at the air. Colloids Surf. A. 116, 173-180.

41. Lalchev, Z. I. and A.R. Mackie 1999. Molecular lateral diffusion in model membrane systems. Colloids Surf. B. 15, 147-160.

42. Mingins, J., D. Stigter and K.A. Dill 1992. Phospholipid interactions in model membrane systems. I. experiments on monolayers. Biophys. J. 61, 1603-1615.

43. Stigter, D., J. Mingins and K.A. Dill 1992. Phospholipid interactions in model membrane systems. II. theory. Biophys. J. 61, 1616-1629.

44. Heimburg, T. 2000. A model for the lipid pretransition: Coupling of ripple formation with the chain-melting transition. Biophys. J. 78, 1154-1165.

45. Feng, Z. V., T.A. Spurlin and A.A. Gewirth 2005. Direct visualization of asymmetric behavior in supported lipid bilayers at the gel-fluid phase transition. Biophys. J. 88, 2154-2164.

46. Charrier, A. and F. Thibaudau 2005. Main phase transitions in supported lipid single-bilayer. Biophys. J. 89, 1094-1101.

47. Ma, G. and H.C. Allen 2006. DPPC langmuir monolayer at the air-water interface: Probing the tail and head groups by vibrational sum frequency generation spectroscopy. Langmuir. 22, 5341-5349.

48. Gunster, J. and R. Souda 2006. On the wettability of lipid DPPC films. Langmuir. 22, 6939-6943.

49. Last JA, A.C. Hillier , D.E. Hooks , J.B. Maxson and M.D Ward 1998. Epitaxially driven assembly of crystalline molecular films on ordered substrates. Chem. Mater. 10, 422-437.

50. Schneider M.F., D. Marsh, W. Jahn, B. Kloesgen, and T. Heimburg 1999 Network formation of lipid membranes: Triggering structural transitions by chain melting. PNAS 1999, 96(25), 14312-14317.

51. Mc Conlogue C.W. and T.K Vanderlick 1997. A close look at domain formation in DPPC monolayers. Langmuir 13 (26), 7158-7164.

52. Hetzer, M., S. Heinz, S. Grage and T.M. Bayerl 1998. Asymmetric molecular friction in supported phospholipid bilayers revealed by NMR measurements of lipid diffusion. Langmuir. 14, 982-984.

53. Nishimura, S., S. Biggs, P.J. Scales, T.W. Healy, K. Tsunematsu and T. Tateyama 1994. Molecular-scale structure of the cation modified muscovite mica basal-plane. Langmuir. 10, 4554-4559.

54. Garcia-Manyes, S., O. Domènech, F. Sanz, M.T. Montero and J. Hernandez-Borrell 2007. Atomic force microscopy and force spectroscopy study of langmuir-blodgett films formed by heteroacid phospholipids of biological interest. Biochim. Biophys. Acta. *accepted.*

55. Schneider J., Y.F. Dufrene, W.R. Barger and G.U. Lee 2000 Atomic force microscope image contrast mechanisms on supported lipid bilayers. Biophys. J. 79 (2): 1107-1118

56. Butt, H. J. 1991. Measuring electrostatic, vanderwaals, and hydration forces in electrolyte-solutions with an atomic force microscope. Biophys. J. 60, 1438-1444.

57. Yang, X. M., D. Xiao, S.J. Xiao and Y. Wei 1994. Domain-structures of phospholipid monolayer langmuir-blodgett-films determined by atomic-force microscopy. Applied Physics A-Materials Science & Processing. 59, 139-143.

58. Schneider, J., W. Barger and G.U. Lee 2003. Nanometer scale surface properties of supported lipid bilayers measured with hydrophobic and hydrophilic atomic force microscope probes. Langmuir. 19, 1899-1907.

59. Pasenkiewicz-Gierula, M., Y. Takaoka, H. Miyagawa, K. Kitamura and A. Kusumi 1999. Charge pairing of headgroups in phosphatidylcholine membranes: A molecular dynamics simulation study. Biophys. J. 76, 1228-1240.

60. PasenkiewiczGierula, M., Y. Takaoka, H. Miyagawa, K. Kitamura and A. Kusumi 1997. Hydrogen bonding of water to phosphatidylcholine in the membrane as studied by a molecular dynamics simulation: Location, geometry, and lipid-lipid bridging via hydrogen-bonded water. J. Phys. Chem. A. 101, 3677-3691.

61. Lindblom, G., G. Oradd and A. Filippov 2006. Lipid lateral diffusion in bilayers with phosphatidylcholine, sphingomyelin and cholesterol - an NMR study of dynamics and lateral phase separation. Chem. Phys. Lipids. 141, 179-184.

62. Bockmann, R. A. and H. Grubmuller 2004. Multistep binding of divalent cations to phospholipid bilayers: A molecular dynamics study. Angewandte Chemie-International Edition. 43, 1021-1024.

63. Sachs, J. N., H. Nanda, H.I. Petrache and T.B. Woolf 2004. Changes in phosphatidylcholine headgroup tilt and water order induced by monovalent salts: Molecular dynamics simulations. Biophys. J. 86, 3772-3782.

64. Merkel, R., E. Sackmann and E. Evans 1989. Molecular friction and epitactic coupling between monolayers in supported bilayers. Journal De Physique. 50, 1535-1555.

65. Johnson, S. J., T.M. Bayerl, D.C. McDermott, G.W. Adam, A.R. Rennie, R.K. Thomas and E. Sackmann 1991. Structure of an adsorbed dimyristoylphosphatidylcholine bilayer measured with specular reflection of neutrons. Biophys. J. 59, 289-294.

66. Koenig, B. W., S. Kruger, W.J. Orts, C.F. Majkrzak, N.F. Berk, J.V. Silverton and K. Gawrisch 1996. Neutron reflectivity and atomic force microscopy studies of a lipid bilayer in water adsorbed to the surface of a silicon single crystal. Langmuir. 12, 1343-1350.

67. Kiessling, V. and L.K. Tamm 2003. Measuring distances in supported bilayers by fluorescence interference-contrast microscopy: Polymer supports and SNARE proteins. Biophys. J. 84, 408-418.

68. Fromherz, P., V. Kiessling, K. Kottig and G. Zeck 1999. Membrane transistor with giant lipid vesicle touching a silicon chip. Applied Physics A-Materials Science & Processing. 69, 571-576.

69. Cremer, P. S. and S.G. Boxer 1999. Formation and spreading of lipid bilayers on planar glass supports. J Phys Chem B. 103, 2554-2559.

70. Kim, J., G. Kim and P.S. Cremer 2001. Investigations of water structure at the solid. Langmuir. 17, 7255-7260.

71. Miranda, P. B., L. Xu, Y.R. Shen and M. Salmeron 1998. Icelike water monolayer adsorbed on mica at room temperature. Phys. Rev. Lett. 81, 5876-5879.

72. Park, S. H. and G. Sposito 2002. Structure of water adsorbed on a mica surface. Phys. Rev. Lett. 89, 085501.

73. Pandit, S. A., D. Bostick and M.L. Berkowitz 2003. Molecular dynamics simulation of a dipalmitoylphosphatidylcholine bilayer with NaCl. Biophys. J. 84, 3743-3750.

74. Israelachvili, J. 1992. Intermolecular and Surface Forces. Academic Press, San Diego.

75. Hui, S. W., D.F. Parsons and M. Cowden 1974. Electron-diffraction of wet phospholipid bilayers. Proc. Natl. Acad. Sci. U. S. A. 71, 5068-5072.

76. Janiak, M. J., D.M. Small and G.G. Shipley 1979. Temperature and compositional dependence of the structure of hydrated dimyristoyl lecithin. J. Biol. Chem. 254, 6068-6078.

77. Ulman, A., J.E. Eilers and N. Tillman 1989. Packing and molecular-orientation of alkanethiol monolayers on gold surfaces. Langmuir. 5, 1147-1152.

78. Barrena, E., C. Ocal and M. Salmeron 2000. Molecular packing changes of alkanethiols monolayers on au(111) under applied pressure. J. Chem. Phys. 113, 2413-2418.

79. Barrena, E., C. Ocal and M. Salmeron 2001. Structure and stability of tilted-chain phases of alkanethiols on au(111). J. Chem. Phys. 114, 4210-4214.

80. Barrena, E., S. Kopta, D.F. Ogletree, D.H. Charych and M. Salmeron 1999. Relationship between friction and molecular structure: Alkylsilane lubricant films under pressure. Phys. Rev. Lett. 82, 2880-2883.

81. Schirmeisen, A. and H. Holscher 2005. Velocity dependence of energy dissipation in dynamic force microscopy: Hysteresis versus viscous damping. Physical Rev. B. 72, 045431.

82. Garcia, R., C.J. Gomez, N.F. Martinez, S. Patil, C. Dietz and R. Magerle 2006. Identification of nanoscale dissipation processes by dynamic atomic force microscopy. Phys. Rev. Lett. 97, 016103.

83. Fraxedas, J., S. Garcia-Manyes, P. Gorostiza and F. Sanz 2002. Nanoindentation: Toward the sensing of atomic interactions. Proc. Natl. Acad. Sci. U. S. A. 99, 5228-5232.

84. Khan. A., J. Philip and P. Hess 2004. Young's modulus of silicon nitride used in scanning force microscope cantilevers. J. Appl. Phys. 95, 1667-1672.

85. Voitchovsky, K., S. Antoranz Contera, M. Kamihira, A. Watts and J.F. Ryan 2006. Differential stiffness and lipid mobility in the leaflets of purple membranes. Biophys. J. 90, 2075-2085.

86. Hantz, E., A. Cao, J. Escaig and E. Taillandier 1986. The osmotic response of large unilamellar vesicles studied by quasi-elastic light-scattering. Biochim. Biophys. Acta. 862, 379-386.

87. Oncins, G., S. Garcia-Manyes and F. Sanz 2005. Study of frictional properties of a phospholipid bilayer in a liquid environment with lateral force microscopy as a function of NaCl concentration. Langmuir. 21, 7373-7379.

88. Kopta, S. and M. Salmeron 2000. The atomic scale origin of wear on mica and its contribution to friction. J. Chem. Phys. 113, 8249-8252.

FIGURES AND TABLES

	R=15nm	R=35nm
Affected molecules (Hertz model)	205	360
E_b (KJ/mol)	0.8	0.5
% broken Van der Waals interactions in a linear rupture (%R_l)	5	4
% broken Van der Waals interactions in a circular rupture(%R_c)	16	11
%(E_b / E_{vdW})	4	3

Table 1. Mechanical and structural parameters of a DPPC monolayer compressed by an AFM tip of radius 15 nm and 35 nm.

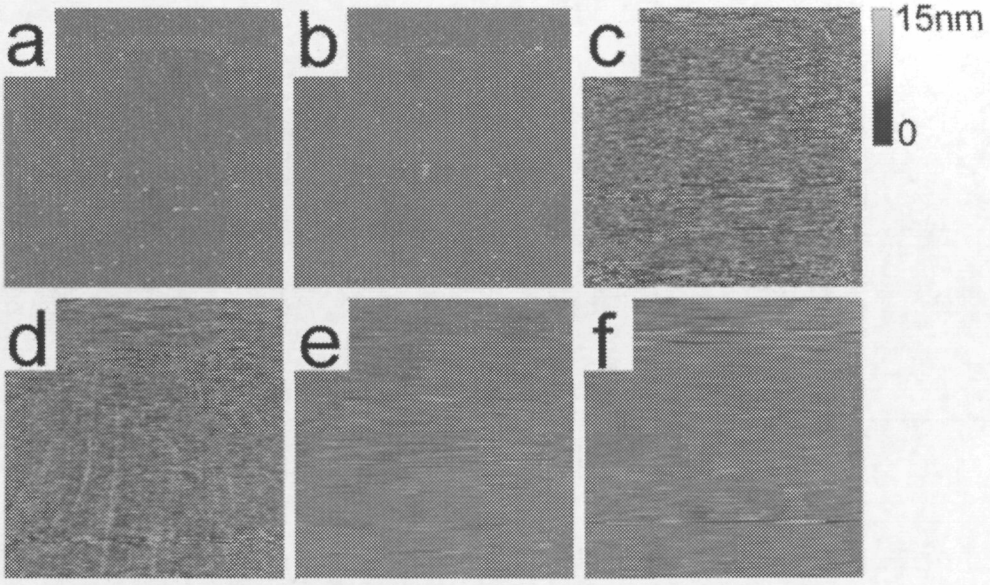

Fig. 1. 5x5 µm AFM tapping images of a DPPC monolayer extracted at 30 mN/m and imaged in buffer solution. The images were obtained at variable temperature; a) 33.1°C; b) 43.6°C; c) 45.4°C; d) 47.8°C.; e) 51.6°C; f) 55.3°C. Images a) and b) correspond to the LC phase, while images c) and d) represent the phase transition. Images e) end f) correspond to the LE phase.

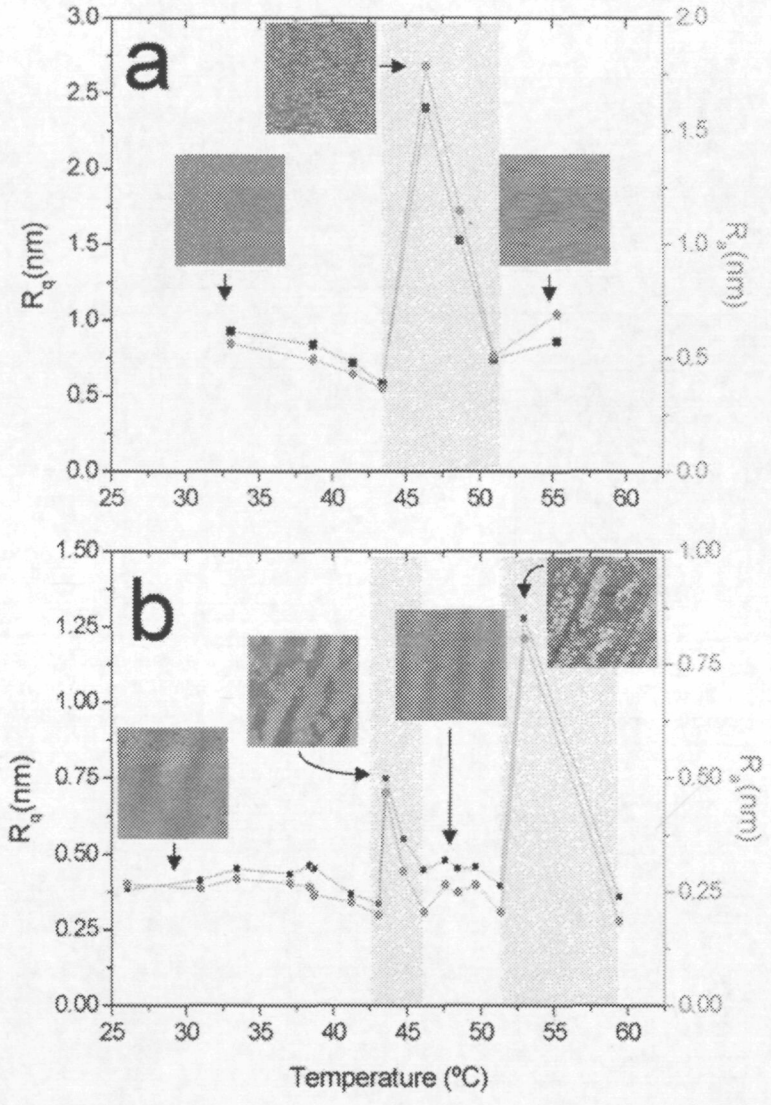

Fig. 2. a) Roughness measurements performed on the topographic images shown in Fig. 1 (DPPC monolayer). Black line-white squares graph corresponds with R_q (left Y-axis) while grey line-black dots graph corresponds with R_a. The roughness increment corresponds with the LC-LE phase transition. b) Roughness measurements of a series of DPPC bilayer topographic images obtained at increasing temperatures. The complete topographic series was presented in a previous work (18). The two roughness increments around 45 and 55°C correspond with the two phase transitions. The grey areas in Fig 2a and 2b enclose the observed transition temperature intervals. All presented images are 5 μm x 5 μm.

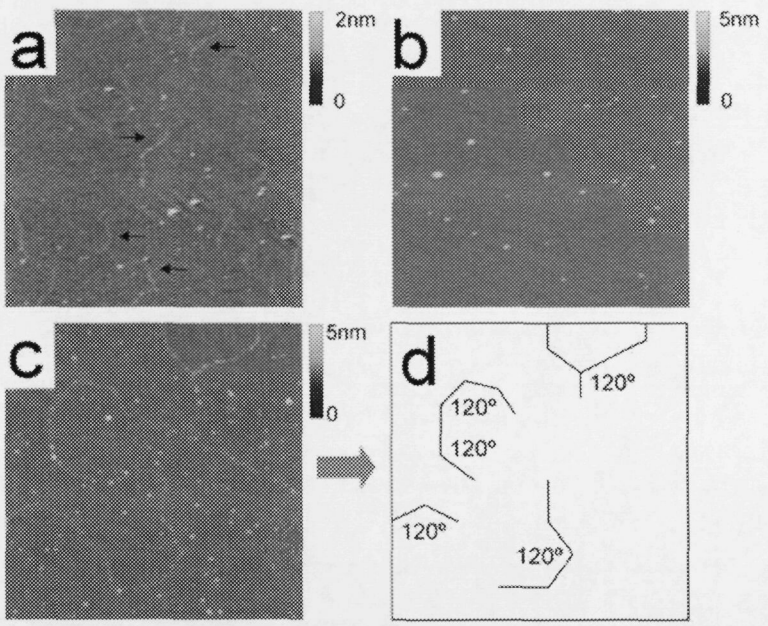

Fig. 3. 2 μm x 2 μm images of DPPC monolayers extracted at 30 mN/m and imaged in air at different temperatures. a) 25°C, below T_M (LC phase); Black arrows point the presence of domain boundaries. b) 65°C, above T_M (LE phase); c) 30°C, below T_M (LC phase). d) Scheme of the domain boundaries observed in Fig. 3c.

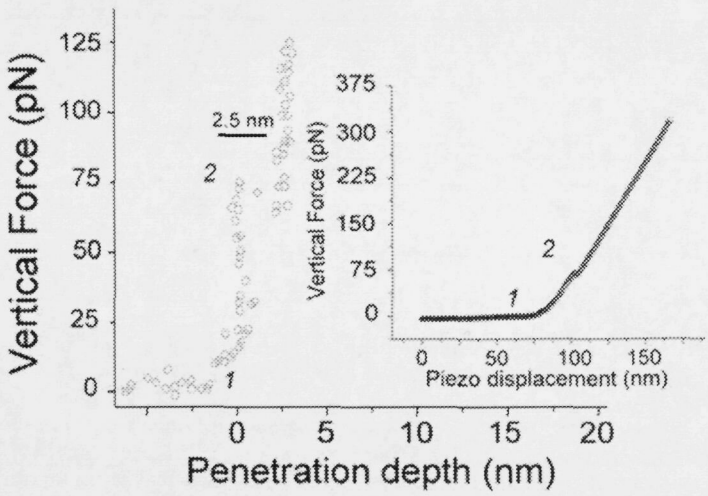

Fig. 4. FvP curve obtained on a DPPC monolayer extracted at 30 mN/m in buffer solution at 46°C. The monolayer breakthrough can be seen around 75 pN. Inset: corresponding FvD curve. (1) corresponds with the contact point and (2) is the monolayer rupture

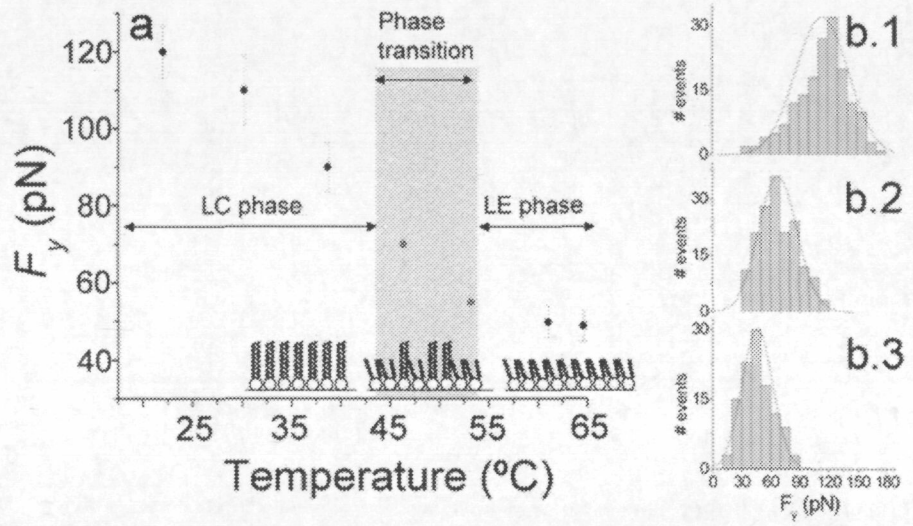

Fig. 5. a) DPPC monolayer F_y vs sample temperature. Each point is the mean value of 150-200 individual breakthrough events detected in force curves. Force curves were performed, at least, in 4 different locations for each temperature. The graph has been divided in three regions according to the monolayer phase. b) Individual histograms of the experimental F_y values at different temperatures. b.1) 21.2°C, b.2) 46.4°C, b.3) 64.7°C.

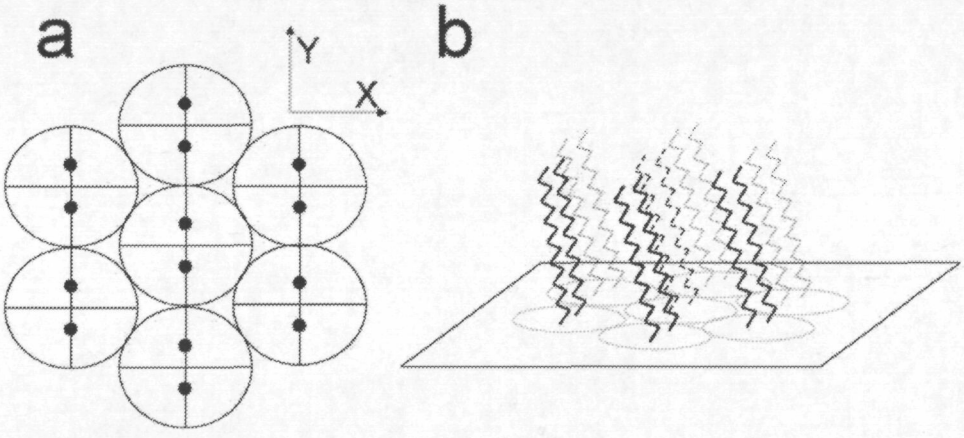

Fig. 6. a) Upper view of the DPPC hexagonal packing. The circles represent the DPPC molecular area and the black dots represent the hydrocarbon chains. b) Lateral view of the same structure. The DPPC hydrocarbon chains are tilted 25° when no vertical load is applied.

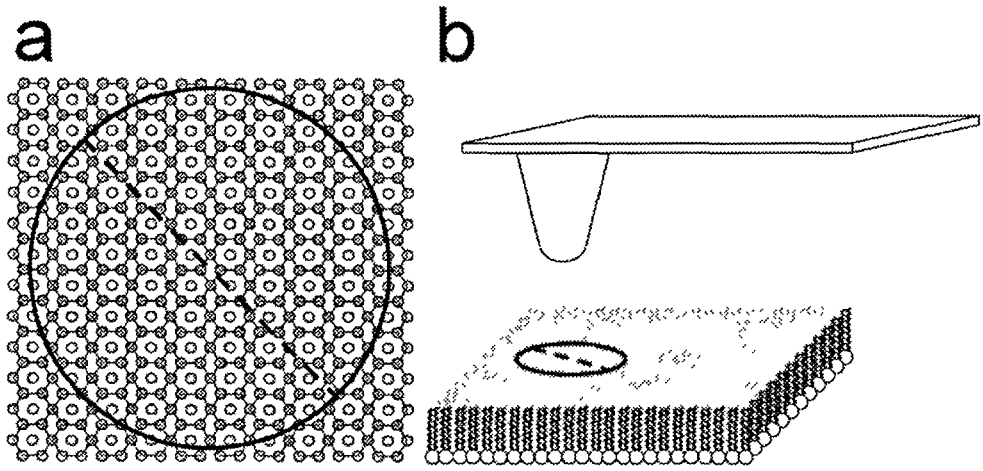

Fig. 7. a) Upper view of a DPPC monolayer hexagonal packing. The black circle encloses the hertzian contact area during a penetration experiment. Two monolayer rupture models are proposed in this work: across a straight line (dotted line) and across the perimeter of the hertzian contact area. b) Lateral view of the same structure.

Chapter 6

6.Conclusions

The conclusions of this work can be structured in two different parts, that is, the conclusions concerning the development and implementation of experimental techniques in our laboratory and the conclusions obtained after applying these techniques to the studied samples. In case more detailed information is required, a summary of the conclusions is also presented before each of the published works attached in the *Experimental Results* sections in Chapters 3, 4 and 5 and also in the *Conclusions* section of each paper.

Concerning the development and implementation of techniques during this PhD thesis, I would like to highlight LFM and Force Spectroscopy, which have been the two key tools that have been used to assess the nanomechanics of organic layers and biomembranes. Regarding LFM, the main development has been the implementation of a home-made electronics card that controls the tip deflection setpoint and provides a continuous variation of its value. This way, F_v vs. F_f curves can be obtained orders of magnitude faster and, provided that this kind of measurements must be performed in several sample spots in order to be statistically meaningful, accurate and representative friction measurements can be reported. Besides, the whole system was adapted to perform measurements in liquid medium, a key experimental factor provided that we wanted to test biomembranes in physiological environment. Finally, the procedures to measure the spring constant of AFM tips both in the vertical and in the lateral directions were successfully implemented and routinely performed in our laboratory.

Concerning Force Spectroscopy, the methodology to obtain reproducible Δx vs. Δz curves was established and applied to the vast majority of the samples studied in this thesis. Due to the large amount of spectroscopic data gathered during experiments, a protocol was established to filter and process the curves and extract F_y values in a more convenient way.

Regarding the experimental results, I will point out a general conclusion for each kind of studied sample.

Engineering coatings

Concerning the nanotribological response of DLC films, humidity increases the μ and the F_f values at a certain F_v, while the different PECVD deposition parameters do not modify them noticeably. Nevertheless, both in humid and dry environment, DLC films provide excellent lubricant layers.

Concerning alkanethiol monolayers on Au(111), the compression studies show that the monolayer deforms in discrete steps which can correspond to the formation of terminal gauche defects or to cooperative molecular foldings. Besides, the F_v necessary to trigger the deformation process strongly depends on the monolayer compactness.

The angle that fatty acid molecules form with the mica substrate depends on the surface pressure of the monolayer, as well as the F_y value (the higher the surface pressure, the higher the F_y value). These results are confirmed by F_f vs. F_v curves, where different tribological regimes are seen as the tip disrupts the monolayer.

Concerning alkanephosphonic acid molecules on aluminum, the monolayers frictional response depends on the substrate, as it determines the molecular bonding sites. The frictional response also depends on the compactness of the monolayers, as the molecular ordering determines the existence of pathways to dissipate the sliding energy.

Concerning the monolayers of Cu(II) sensor tiomacrocycle on mica, the structural morphology and nanotribological response of the monolayers strongly depends on the Langmuir film extraction pressure.

As you can see, several factors determine the nanomechanical properties of the monolayers: the extraction surface pressure (in case of LB films), the nature of the substrate in the case of molecules covalently bonded to it and the monolayer compactness because molecules can change their orientation and, consequently, their resistance to be penetrated or laterally dragged by an AFM tip.

Biomembranes

The effect of pH and ionic strength on the phospholipid bilayers structure was explored by means of nanomechanics techniques. Both using Force Spectroscopy and LFM, it is clear that the bilayers compactness increases with the presence of ions, as the necessary F_v value to penetrate or disrupt them increases with the ionic concentration. The pH of the medium modifies the surface charge of phospholipid liposomes and is a key factor in order to control their deposition and SPBs formation.

Concerning the phase transition of phospholipid SPBs, variable temperature AFM and Force Spectroscopy are suitable techniques to *in-situ* explore the topographical and nanomechanical changes that these structures undergo. While the main phase transition process of PC bilayers supported on mica shows two individual phase transitions, the liposomes only show one, as is the case for PC LB monolayers. According to that, we conclude that the two transitions observed in the bilayer correspond to the individual melting of the phospholipid leaflets. Due to the high sensitivity of Force Spectroscopy to structural membrane differences, the changes of F_y vs. temperature provide valuable information about the phase transition mechanism and the overall mechanical stability of the studied monolayers and bilayers.